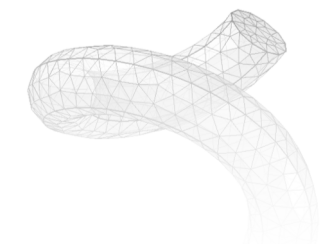
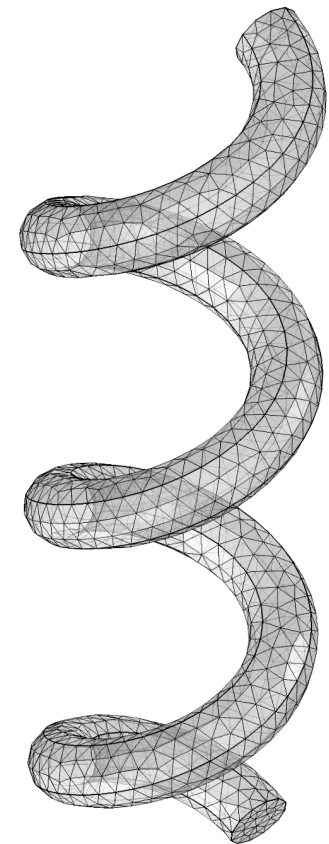


Magnetic Analysis of Ferromagnetic Helical Microstructures

Michel Heusser

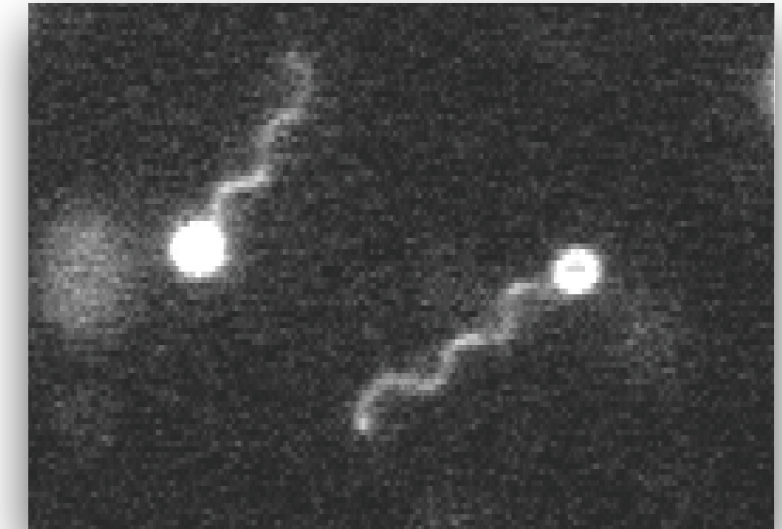
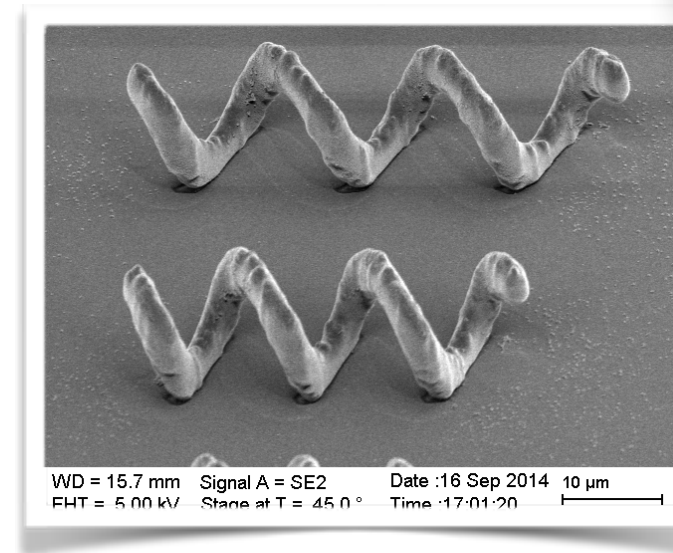
Advisors: Naveen Shamsudhin, Andrew Petruska

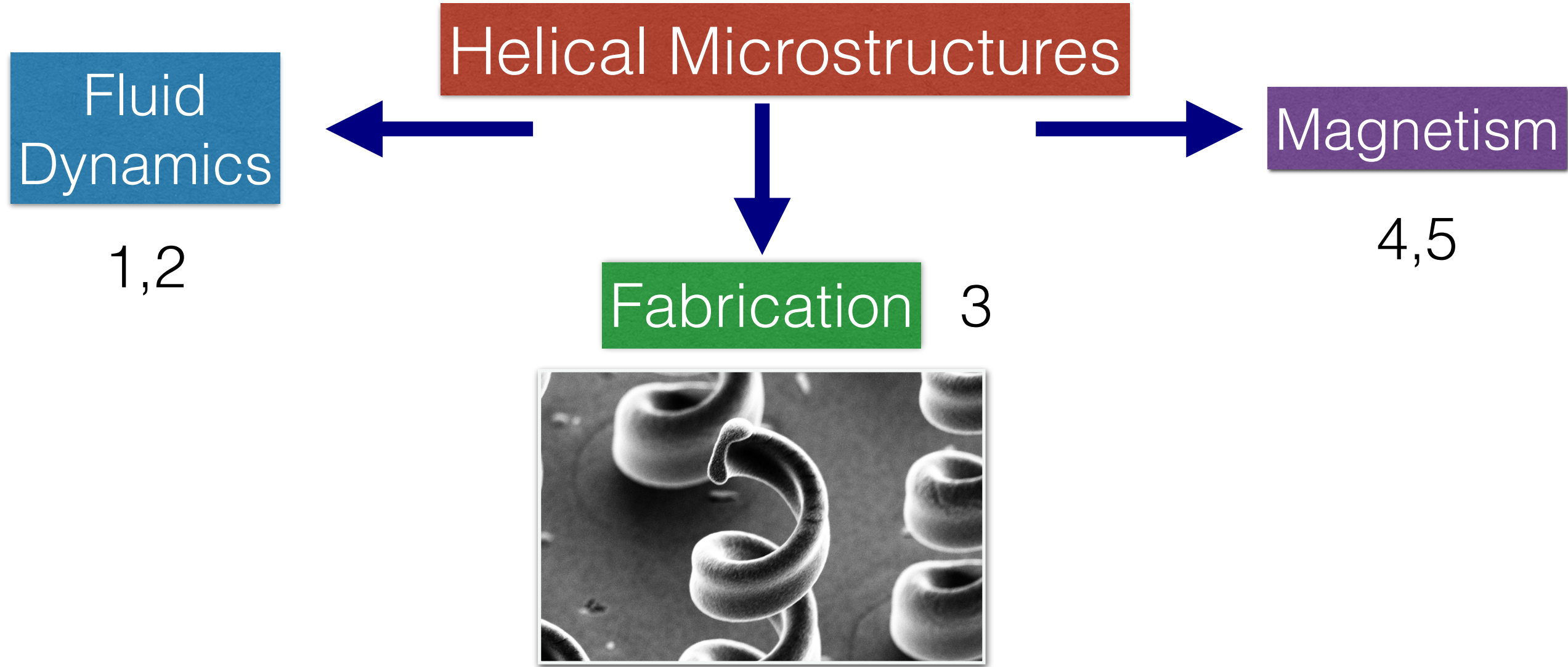
6 July 2015



Magnetic Helical Microstructures

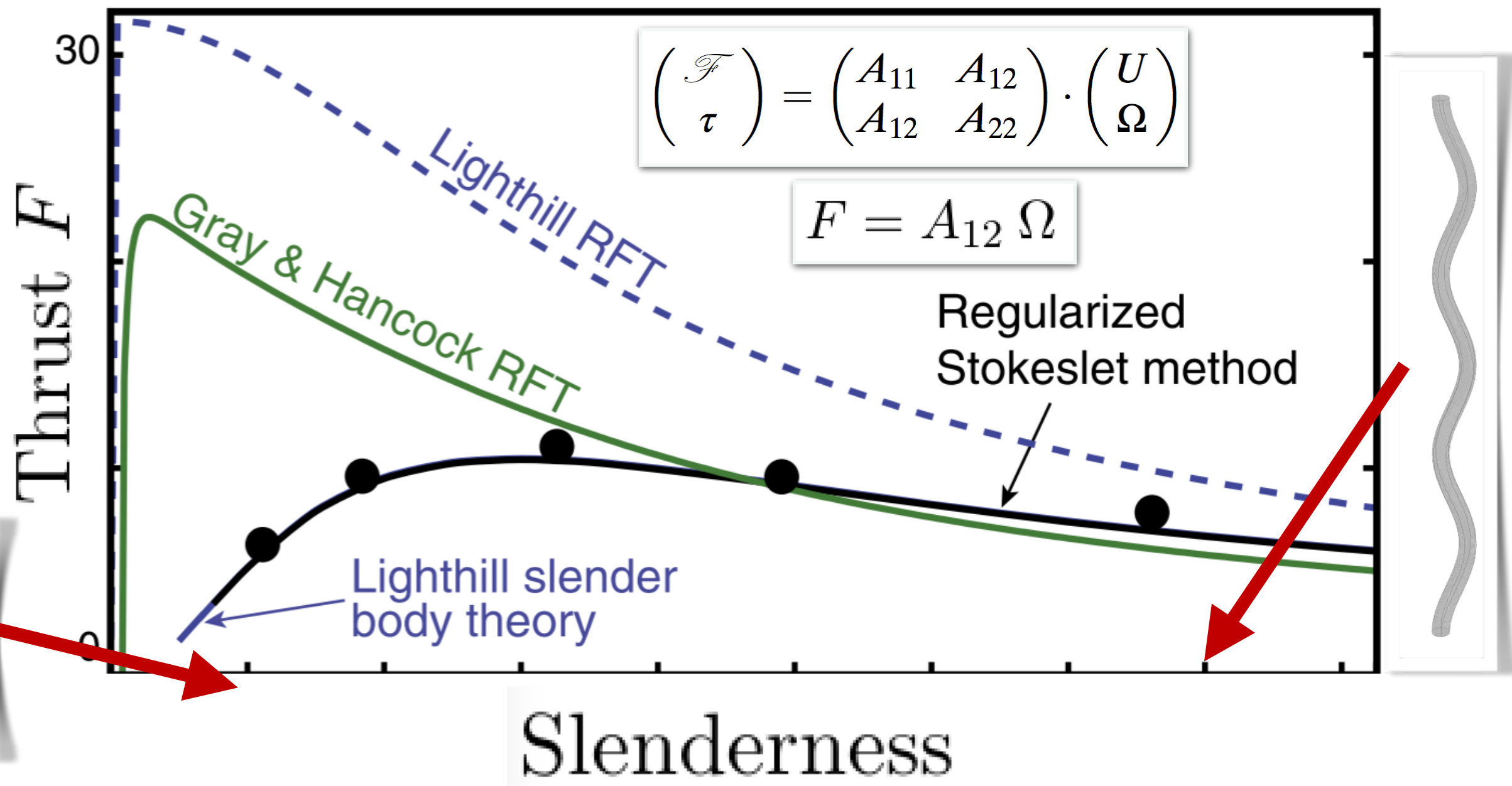
- Uses:
 - Drug delivery
 - Tissue Manipulation
 - Diagnostic & Sensing
- Advantages:
 - No chemical fuels
 - Propulsion through magnetic field (tissue permeability)
 - Rotating field allows micro-scaling (no need of high fields)





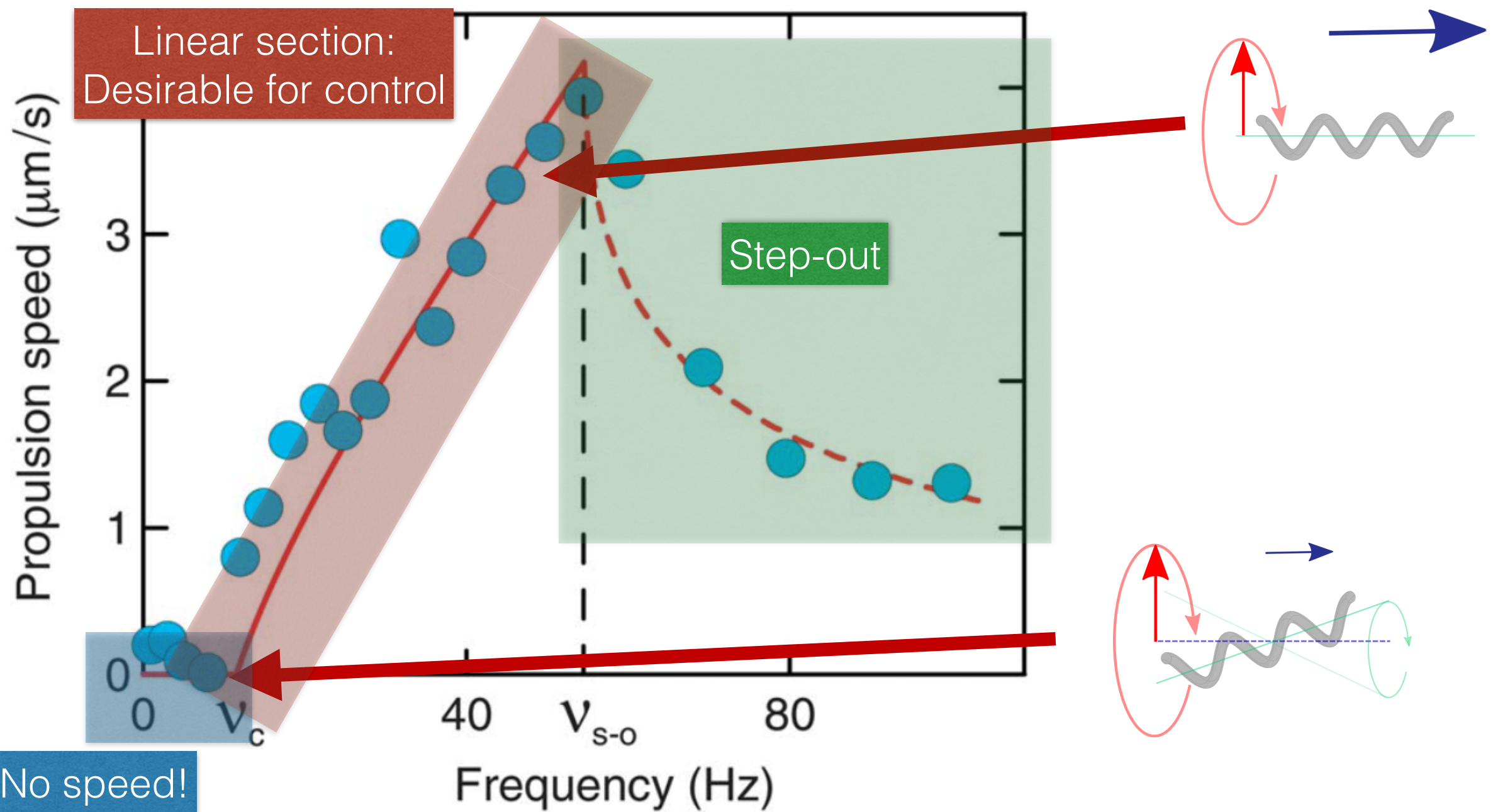
- 1 Morozov, K. I., & Leshansky, A. M. (2014). The chiral magnetic nanomotors. *Nanoscale*, 6(3), 1580–8. doi:10.1039/c3nr04853e
- 2 Rodenborn B, Chen C-H, Swinney HL, Liu B, Zhang HP. Propulsion of microorganisms by a helical flagellum. *Proceedings of the National Academy of Sciences of the United States of America*. 2013;110(5):E338-E347. doi:10.1073/pnas.1219831110.
- 3 Tottori, S., Zhang, L., Qiu, F., Krawczyk, K. K., Franco-Obregón, A., & Nelson, B. J. (2012). Magnetic helical micromachines: fabrication, controlled swimming, and cargo transport. *Advanced Materials* (Deerfield Beach, Fla.), 24(6), 811–6. doi:10.1002/adma.201103818
- 4 Fu, H. C., Jabbarzadeh, M., & Meshkati, F. (2015). Magnetization directions and geometries of helical microswimmers for linear velocity-frequency response. *Physical Review E*, 91, 1–13. doi:10.1103/PhysRevE.91.043011
- 5 Morozov, K. I., & Leshansky, A. M. (2014). Dynamics and polarization of superparamagnetic chiral nanomotors in a rotating magnetic field. *Nanoscale*, 6(20), 12142–50. doi:10.1039/c4nr02953d

Hydrodynamic Shape Effect



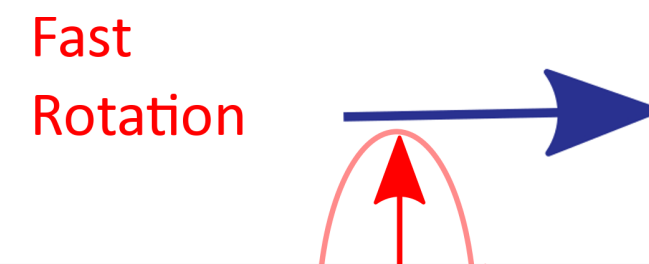
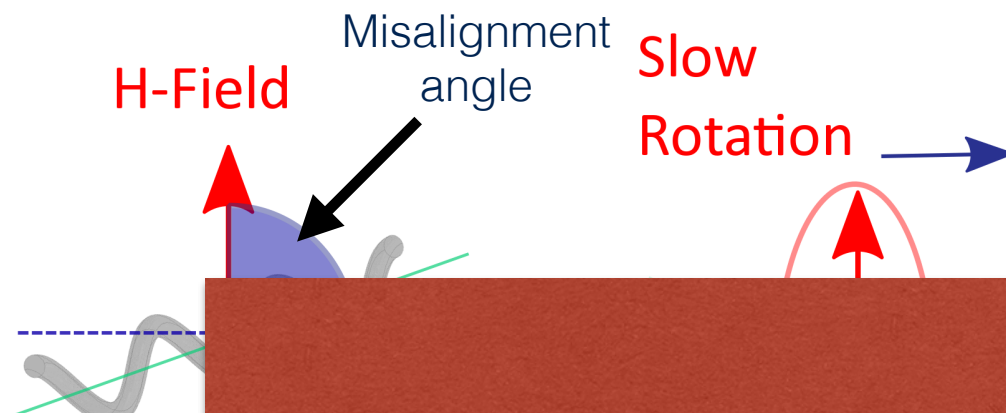
Rodenborn B, Chen C-H, Swinney HL, Liu B, Zhang HP. Propulsion of microorganisms by a helical flagellum. *Proceedings of the National Academy of Sciences of the United States of America*. 2013;110(5):E338-E347. doi:10.1073/pnas.1219831110.

Propulsion Speed vs Frequency



Morozov, K. I., & Leshansky, A. M. (2014). The chiral magnetic nanomotors. *Nanoscale*, 6(3), 1580–8. doi:10.1039/c3nr04853e

Misalignment



Align

Objective:

Finding the magnetically optimal
helical geometry

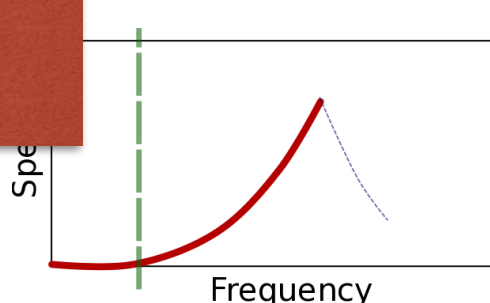
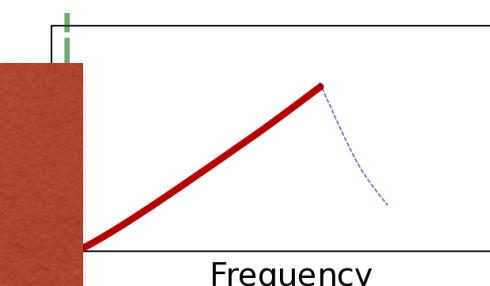


Alignment

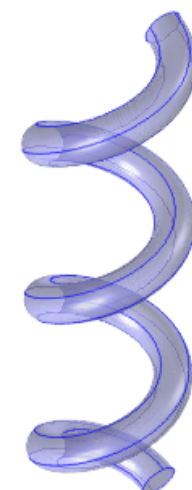
Tumbling

Wobbling

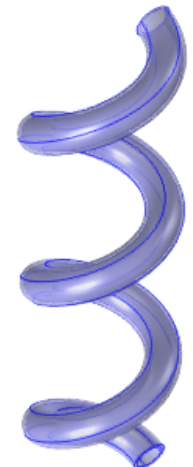
Linear Speed



Types of Helix



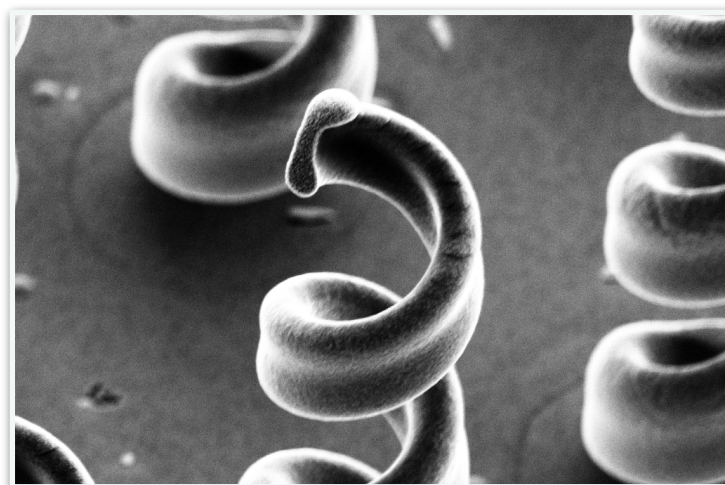
Full
magnetic



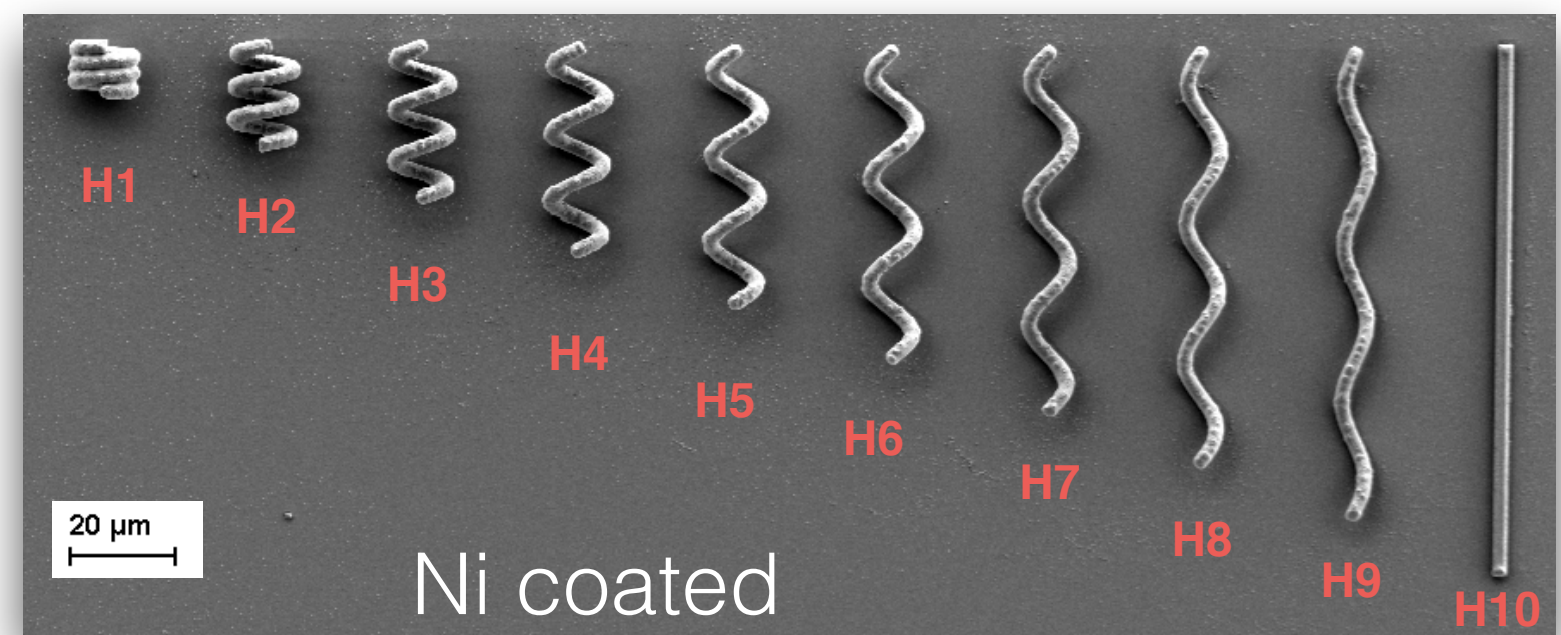
Thin
coated



Half
coated

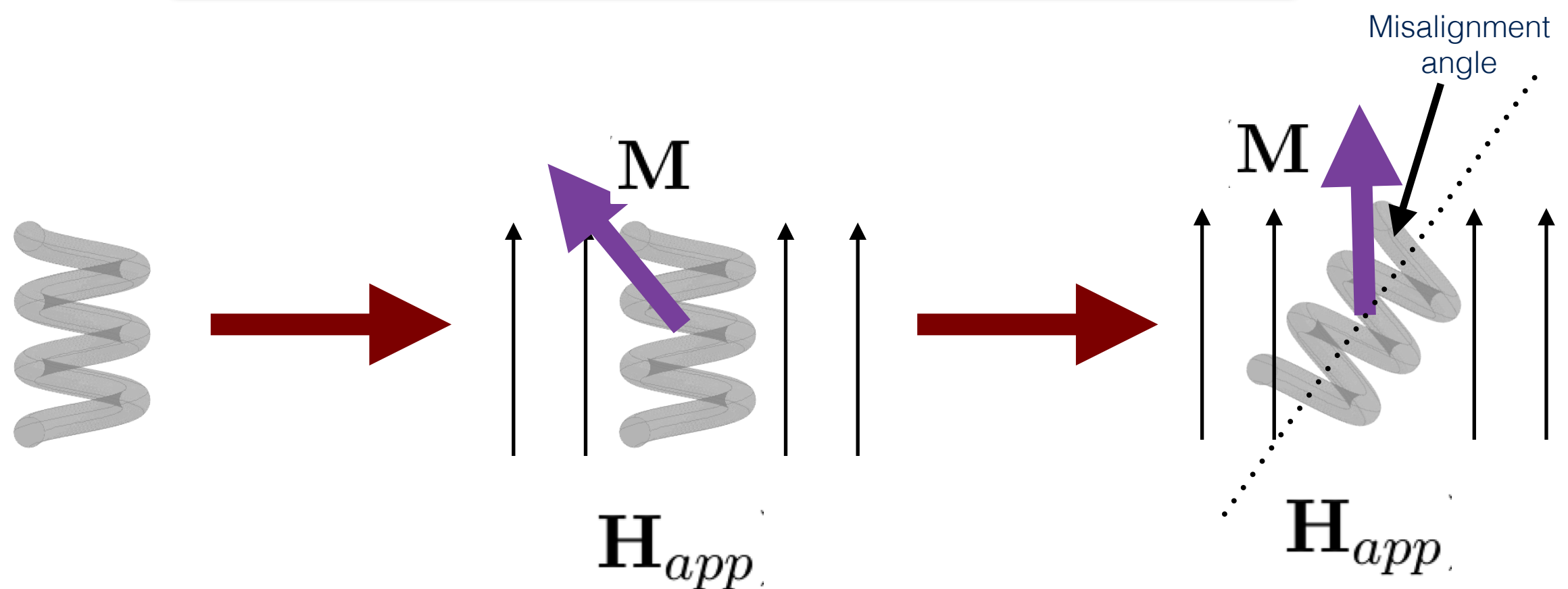


Electro plated



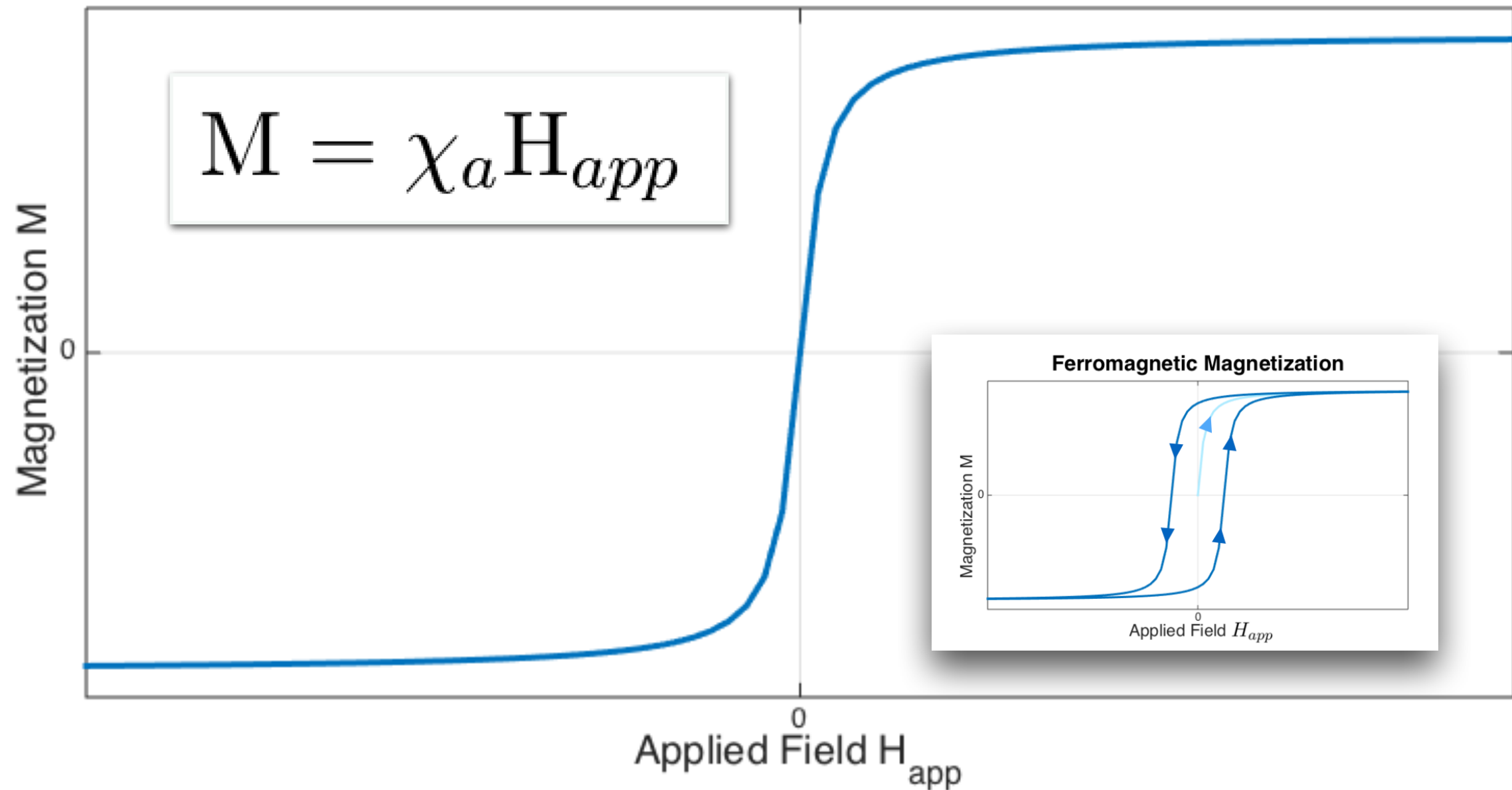
Magnetism

$$\mathbf{T} = \mu_0 V (\mathbf{M} \times \mathbf{H}_{app})$$

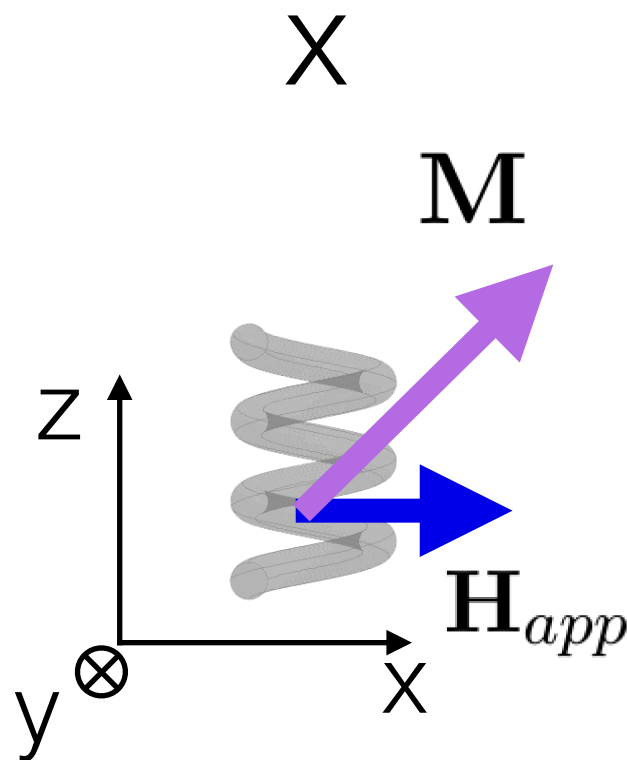


How does a body magnetize?

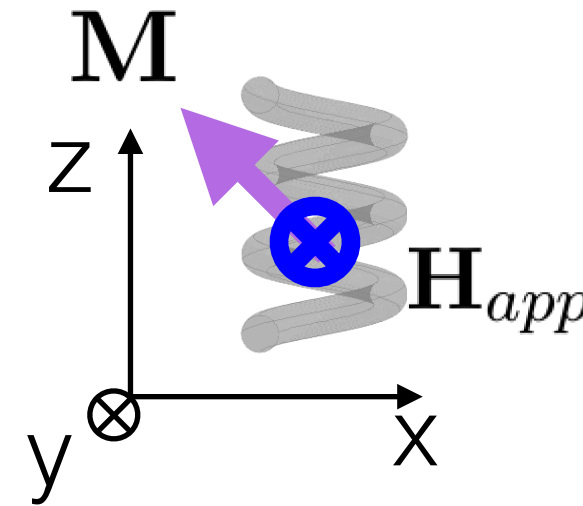
Soft Magnetic Magnetisation



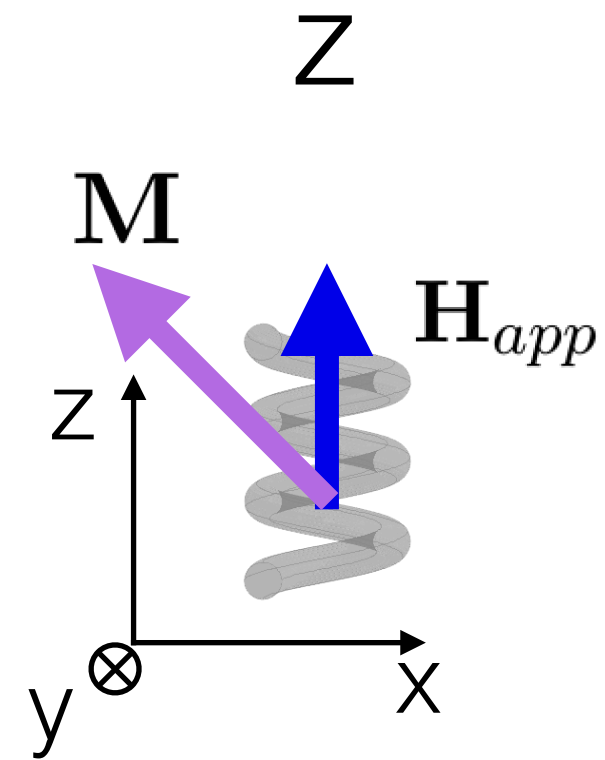
$$\mathbf{M} = \chi_a \mathbf{H}_{app}$$



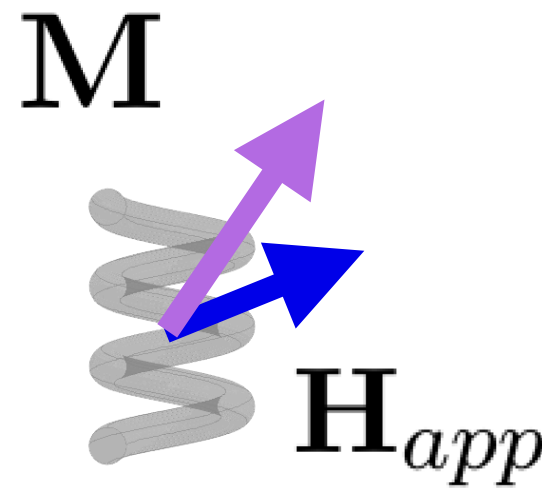
$$\begin{aligned}\mathbf{M}_x &= \chi_{a,xx} \mathbf{H}_{app,x} \\ \mathbf{M}_y &= \chi_{a,xy} \mathbf{H}_{app,x} \\ \mathbf{M}_z &= \chi_{a,xz} \mathbf{H}_{app,x}\end{aligned}$$



$$\begin{aligned}\mathbf{M}_x &= \chi_{a,yx} \mathbf{H}_{app,y} \\ \mathbf{M}_y &= \chi_{a,yy} \mathbf{H}_{app,y} \\ \mathbf{M}_z &= \chi_{a,yz} \mathbf{H}_{app,y}\end{aligned}$$



$$\begin{aligned}\mathbf{M}_x &= \chi_{a,zx} \mathbf{H}_{app,z} \\ \mathbf{M}_y &= \chi_{a,zy} \mathbf{H}_{app,z} \\ \mathbf{M}_z &= \chi_{a,zz} \mathbf{H}_{app,z}\end{aligned}$$



$$\mathbf{M} = \begin{pmatrix} \chi_{a,xx} & \chi_{a,yx} & \chi_{a,zx} \\ \chi_{a,xy} & \chi_{a,yy} & \chi_{a,zy} \\ \chi_{a,xz} & \chi_{a,yz} & \chi_{a,zz} \end{pmatrix} \mathbf{H}_{app}$$

$$\mathbf{M} = \chi_a \mathbf{H}_{app}$$

$$\chi_a = \begin{pmatrix} \chi_{a,xx} & \chi_{a,yx} & \chi_{a,zx} \\ \chi_{a,xy} & \chi_{a,yy} & \chi_{a,zy} \\ \chi_{a,xz} & \chi_{a,yz} & \chi_{a,zz} \end{pmatrix}$$

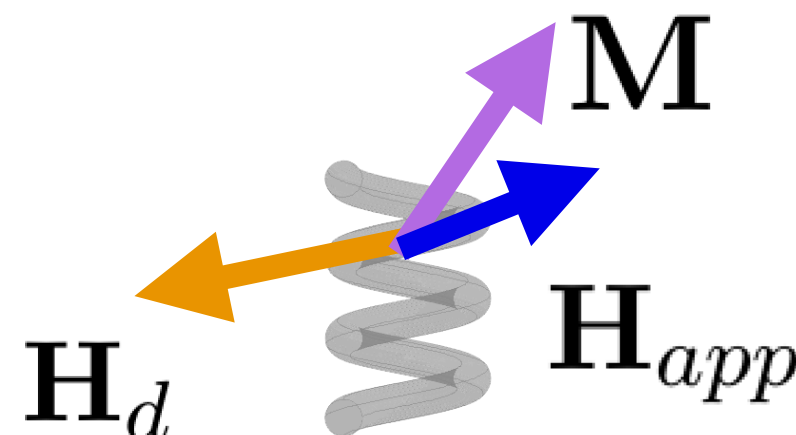
Eigenvectors:
Called “easy axes”

$$\theta = \arccos(\mathbf{v}_{max} \cdot \mathbf{e}_z)$$

Misalignment
angle

Eigenvector
with largest eigenvalue

Demagnetisation



$$\mathbf{H}_d = -N \mathbf{M}$$

$$\mathbf{H} = \mathbf{H}_{app} + \mathbf{H}_d$$

$$\mathbf{M} = \chi_m \mathbf{H}$$

$$\mathbf{M} = \left(\frac{1}{\chi_m} \mathbb{I} + N \right)^{-1} \mathbf{H}_{app}$$

$$\chi_a = \left(\frac{1}{\chi_m} \mathbb{I} + N \right)^{-1}$$

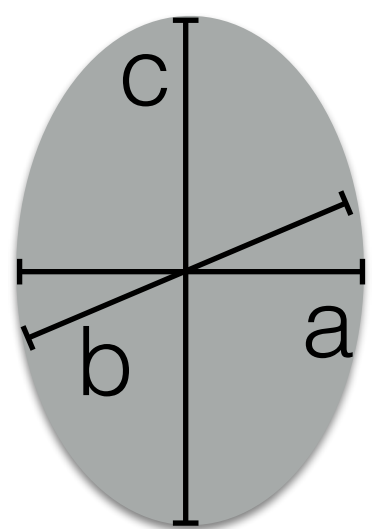
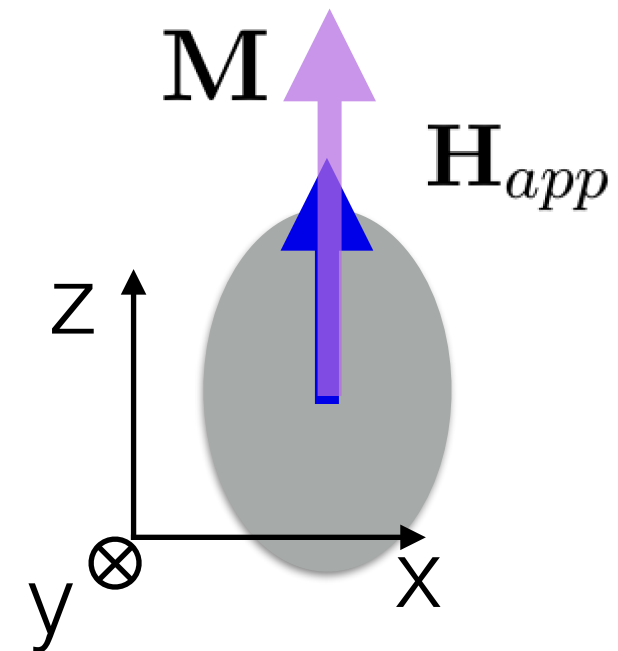
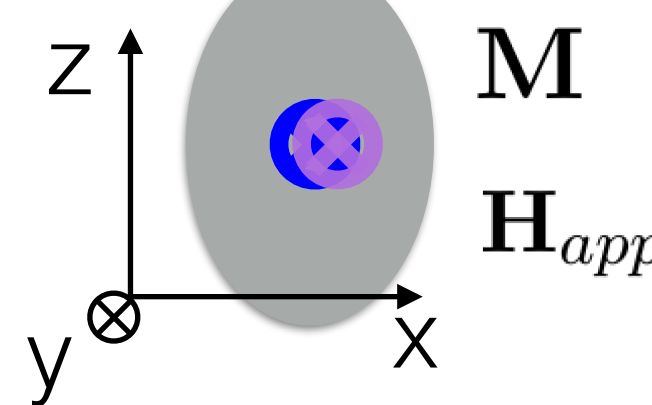
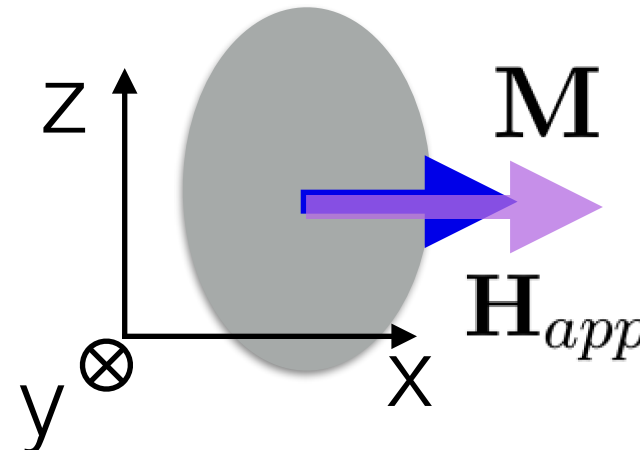
$$\chi_a \approx N^{-1}$$

$$\chi_m \gg 1$$

$$N \leftrightarrow \chi_a$$

Share eigenvectors
Eigenvalues are inverted

Ellipsoids



$$\chi_a = \begin{pmatrix} \chi_{a,xx} & 0 & 0 \\ 0 & \chi_{a,yy} & 0 \\ 0 & 0 & \chi_{a,zz} \end{pmatrix} \quad N = \begin{pmatrix} N_{xx} & 0 & 0 \\ 0 & N_{yy} & 0 \\ 0 & 0 & N_{zz} \end{pmatrix}$$

$$\theta = \arccos(\mathbf{v}_{max} \cdot \mathbf{e}_z)$$

Always the longest semi-axis

Simulation (Fields) vs Analytical (Ellipsoid)

N_simulationM =

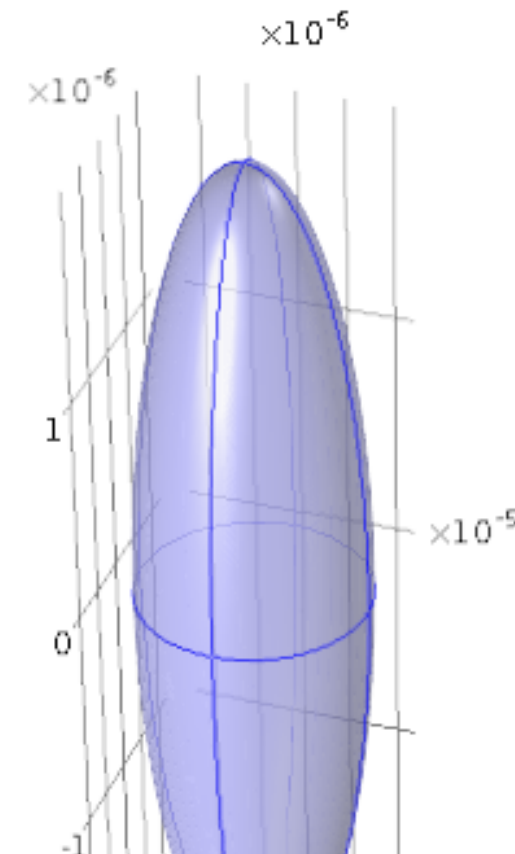
$$\begin{matrix} 0.4629 & 0.0000 & -0.0000 \\ 0.0000 & 0.4629 & 0.0000 \\ 0.0000 & 0.0000 & 0.0738 \end{matrix}$$

N_simulationB =

$$\begin{matrix} 0.4627 & -0.0000 & 0.0002 \\ -0.0001 & 0.4628 & 0.0000 \\ 0.0000 & -0.0000 & 0.0744 \end{matrix}$$

N_analytical =

$$\begin{matrix} 0.4628 & 0 & 0 \\ 0 & 0.4628 & 0 \\ 0 & 0 & 0.0745 \end{matrix}$$

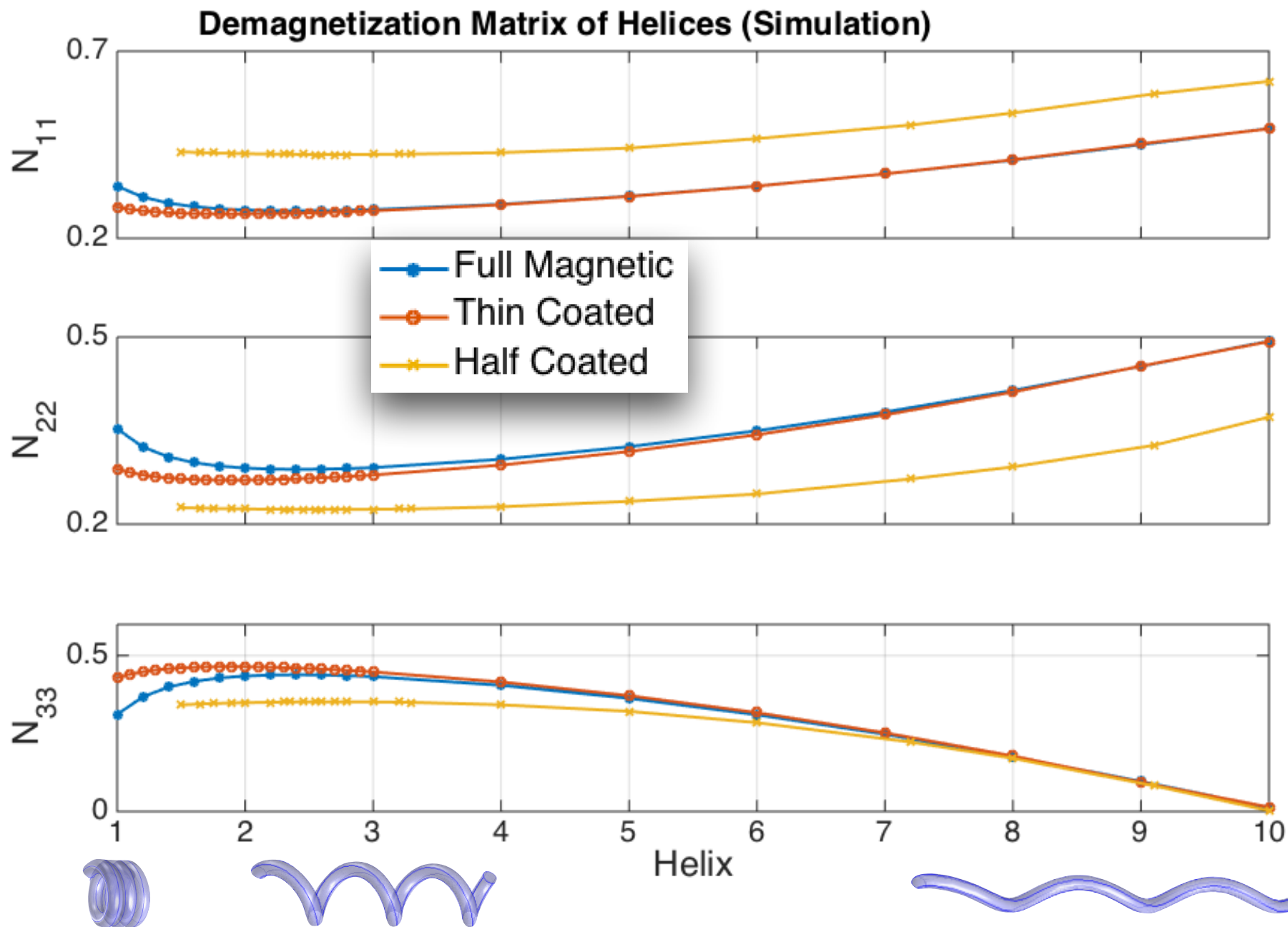


$$N_z(\tau_a, \tau_b) = \frac{1}{\tau_a \tau_b} \frac{F(k, m) - E(k, m)}{m \sin^3 k}$$

$$\begin{aligned} \tau_a &= c/a & k &= \arcsin \sqrt{1 - \tau_a^{-2}} & m &= \frac{1 - \tau_b^{-2}}{1 - \tau_a^{-2}} \\ \tau_b &= c/b \end{aligned}$$

Beleggia, M., Graef, M. De, & Millev, Y. T. (2006). The equivalent ellipsoid of a magnetized body. Journal of Physics D: Applied Physics. doi: 10.1088/0022-3727/39/5/001

Simulation of Helices (High Fields)

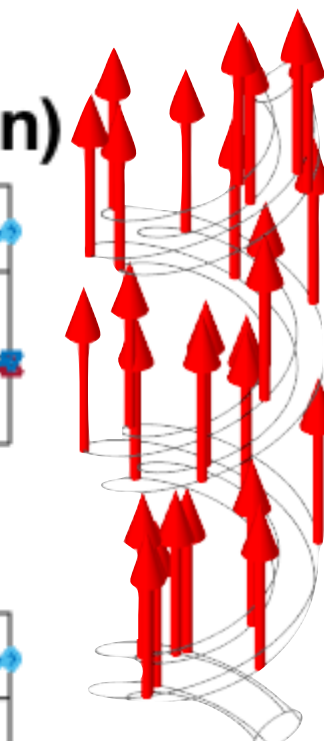
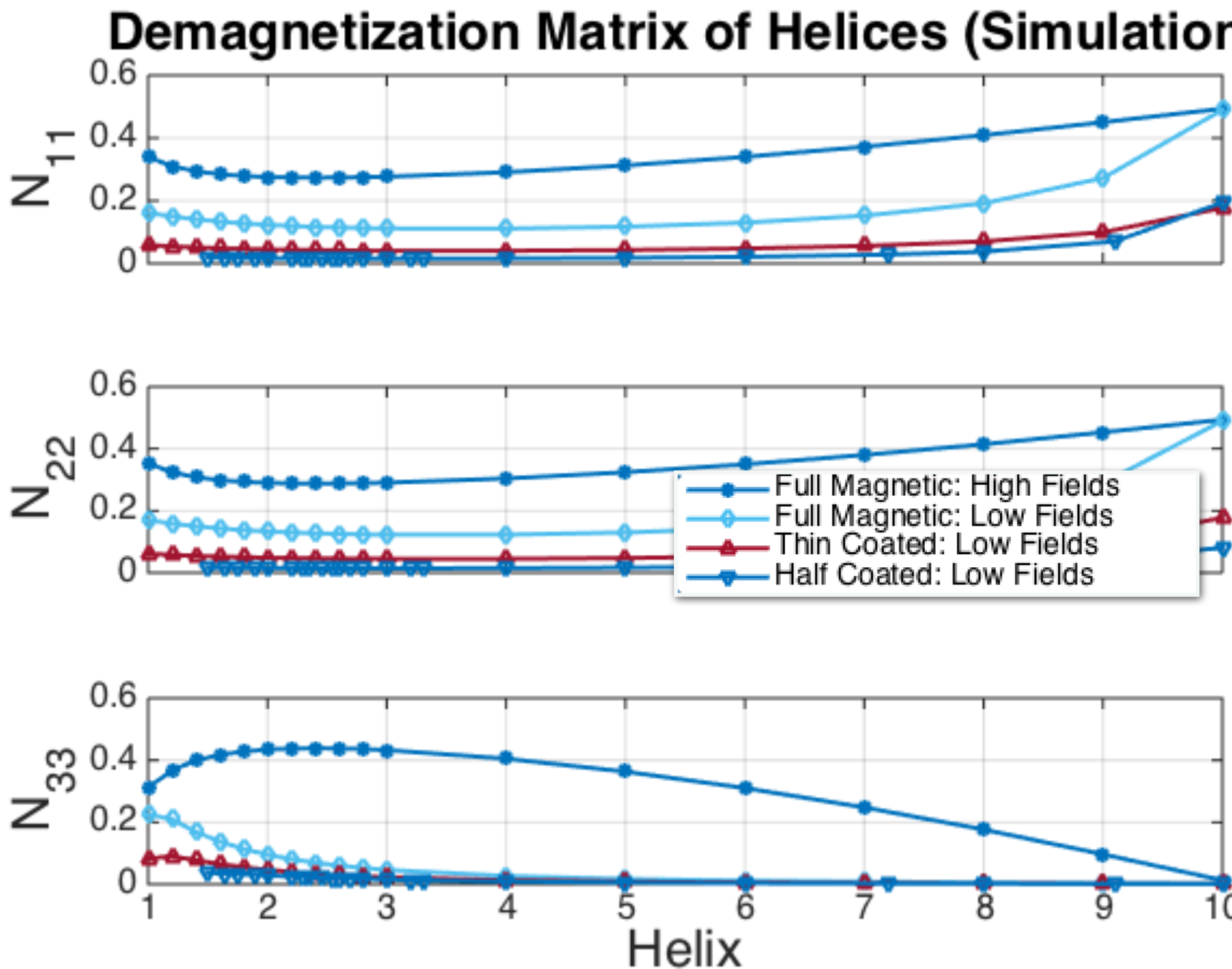


$$N = \begin{pmatrix} 0.2766 & 0.0000 & -0.0000 \\ 0.0000 & 0.2907 & 0.0077 \\ -0.0000 & 0.0077 & 0.4325 \end{pmatrix}$$

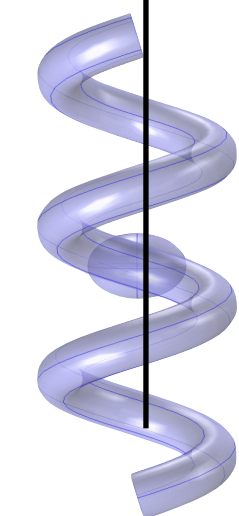
H3

$$N = \begin{pmatrix} N_{11} & N_{21} & N_{31} \\ N_{12} & N_{22} & N_{32} \\ N_{13} & N_{23} & N_{33} \end{pmatrix}$$

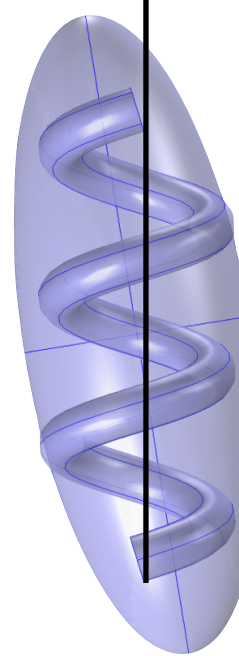
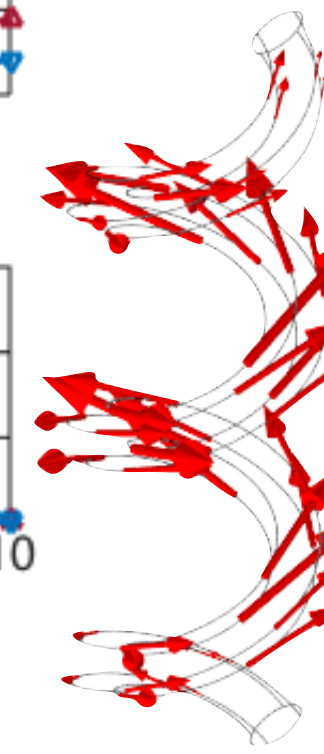
Simulation of Helices (Low Fields)



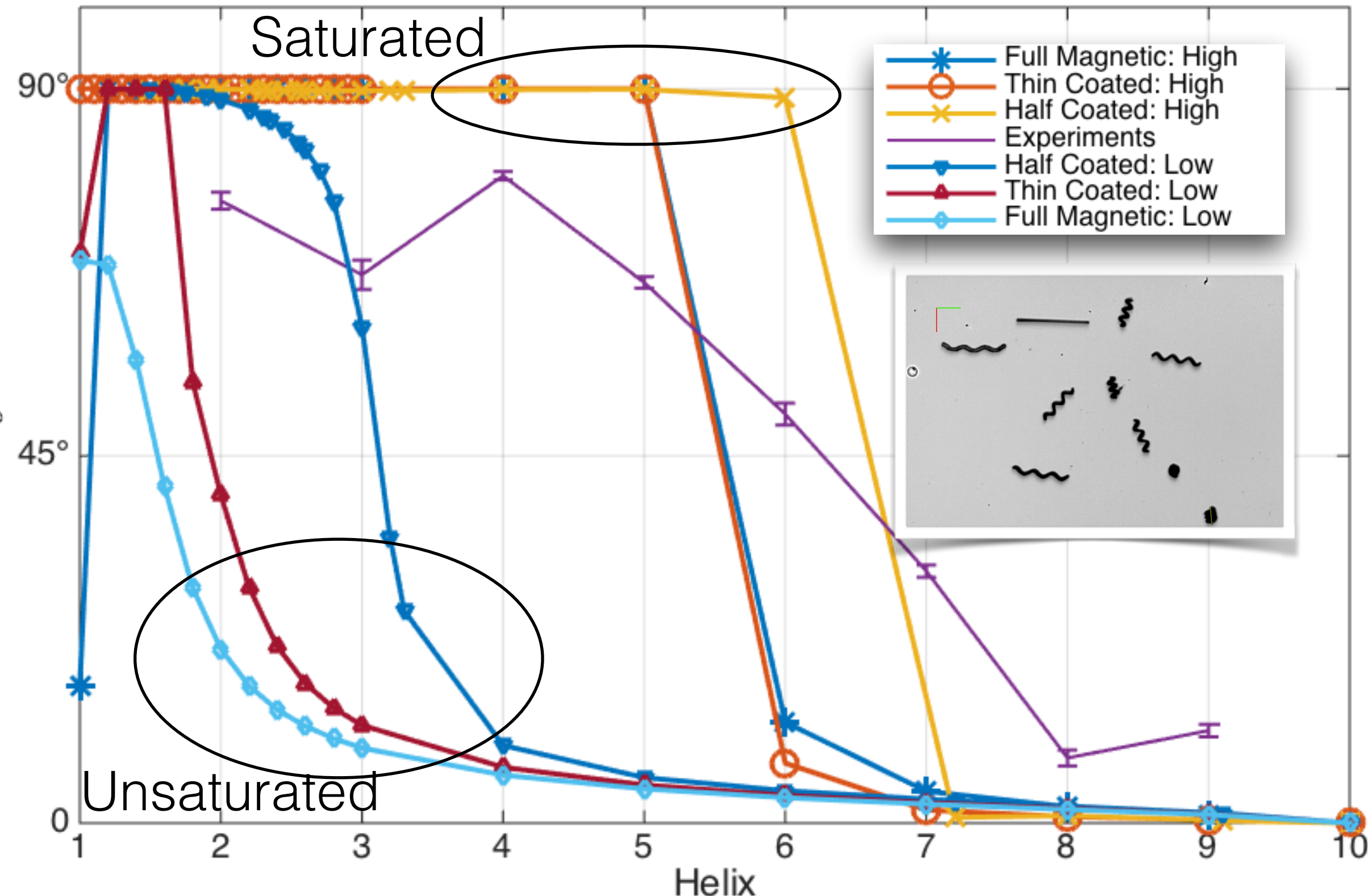
High Fields



Low Fields



Misalignment Angle for Helices



Analytical Model vs FEM

- Both rely on numerical methods
- Analytical model potentially faster
 - Reduced domain for evaluation
 - Through suitable assumptions, simplification of the problem
- More suitable for control purposes

Maxwell Equations (Magnetostatics)

$$\nabla \times \mathbf{H} = 0 \quad \Leftrightarrow \quad \mathbf{H} = -\nabla\psi$$

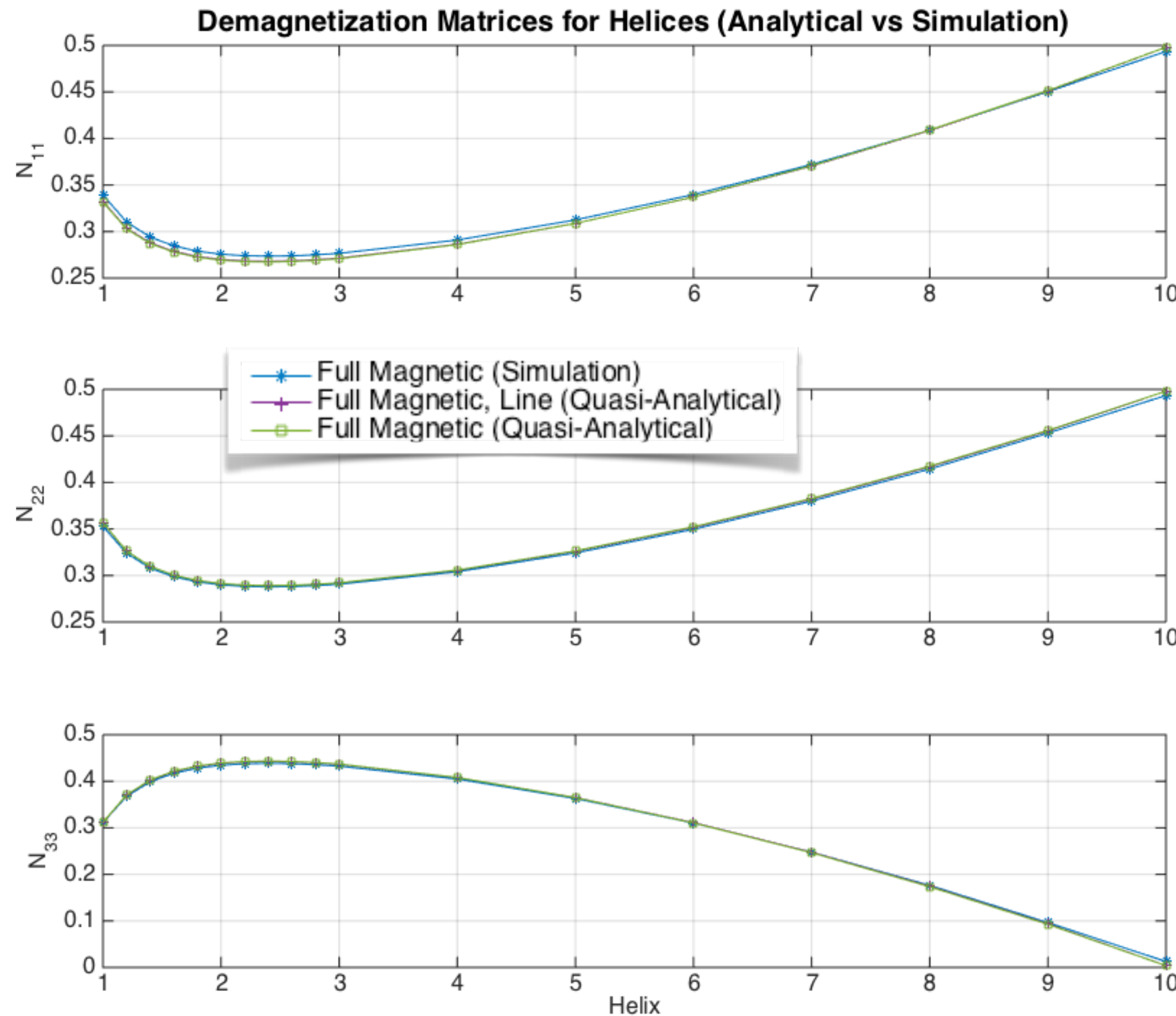
$$\nabla \cdot \mathbf{H} = -\nabla \cdot \mathbf{M}$$

Given external applied field



Given magnetisation

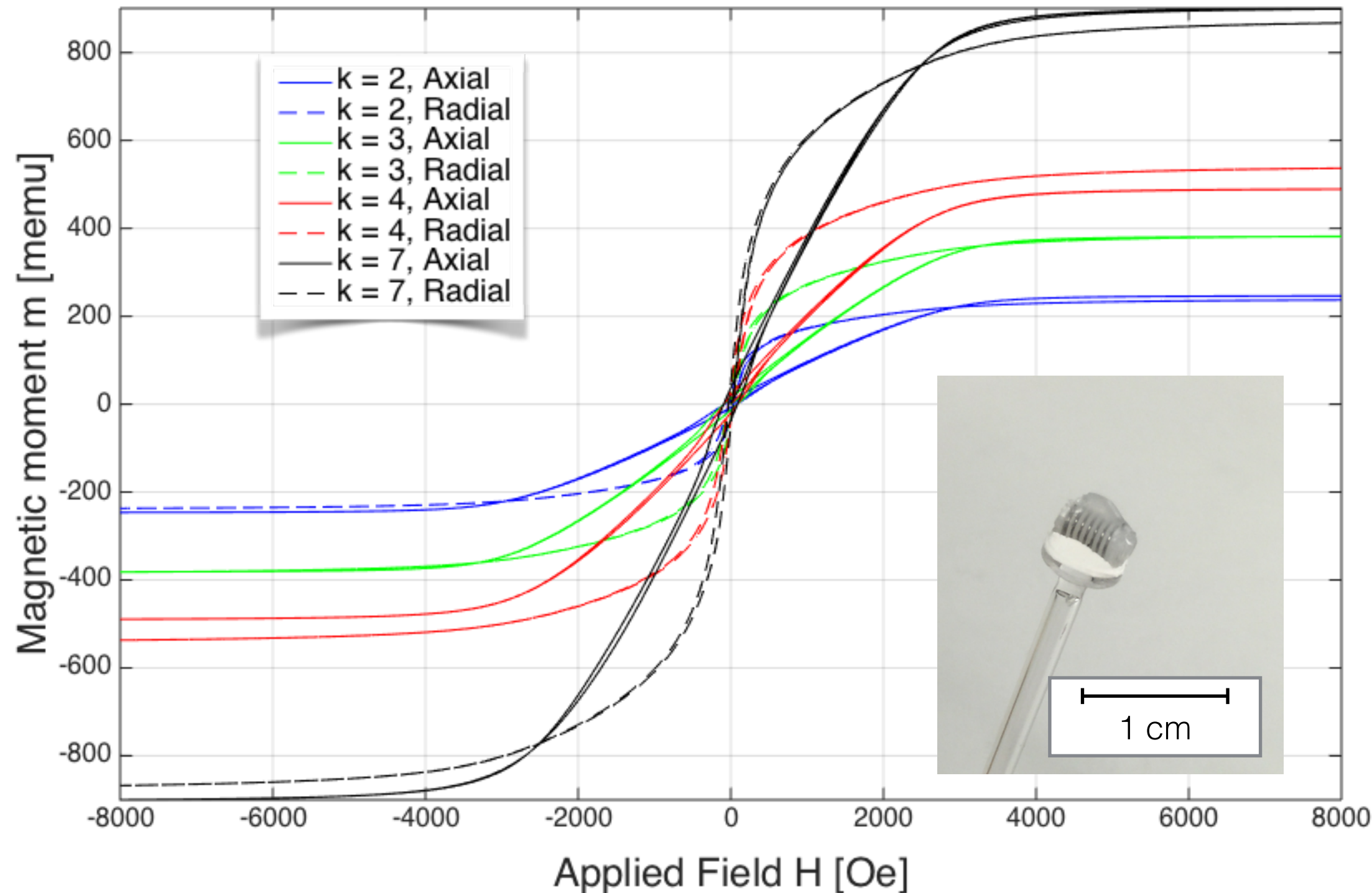
$$\mathbf{H}(\mathbf{r}) = -\frac{1}{4\pi} \int_V \left(\mathbf{n}(\mathbf{r}') \frac{(\mathbf{r}' - \mathbf{r})^T}{|\mathbf{r}' - \mathbf{r}|^3} \right) \mathbf{M}(\mathbf{r}') d^3r' + \mathbf{H}_{app}$$



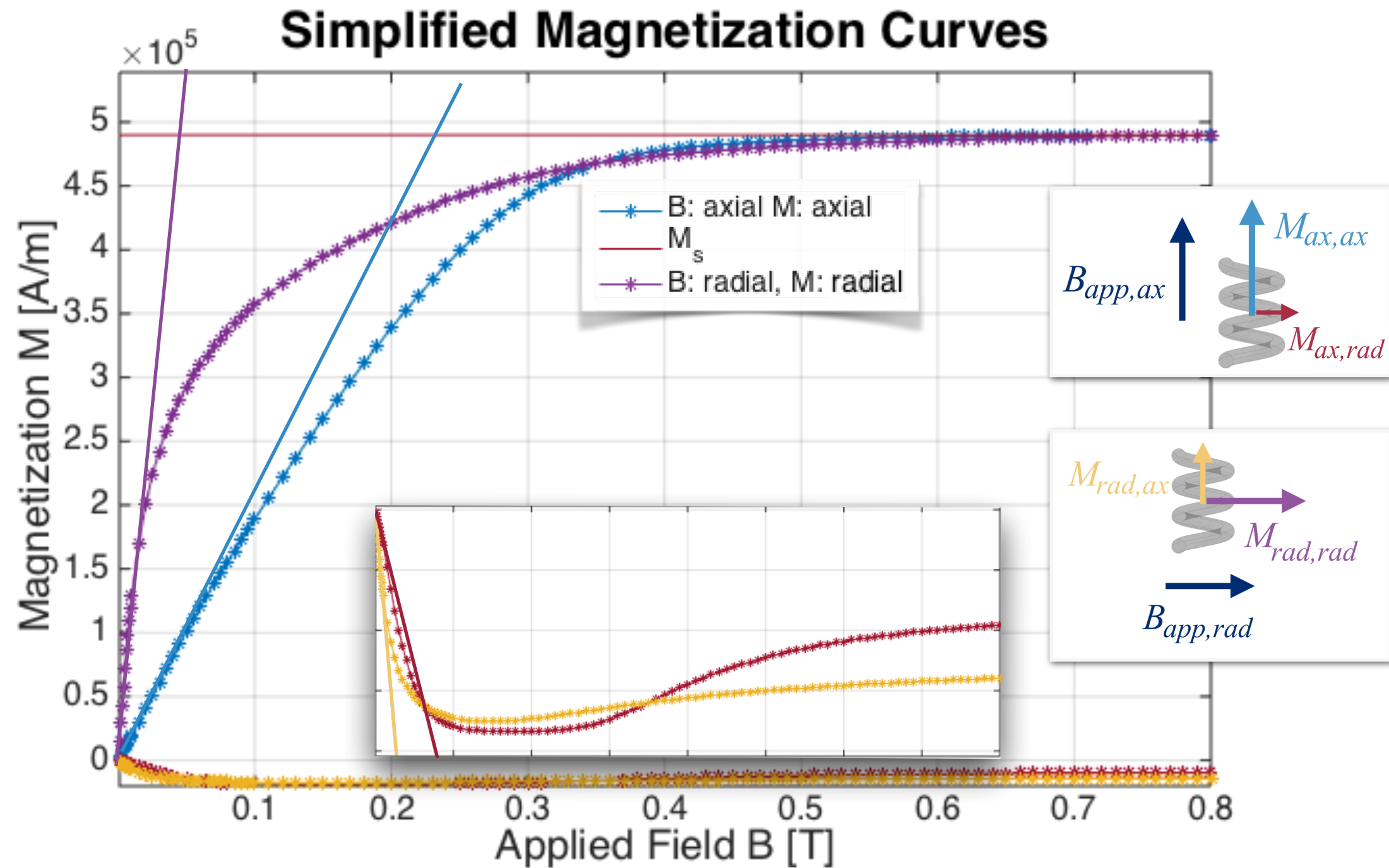
VSM Experiments

- Validation of full magnetic helical magnetisation
- Manually wired nickel macro helices
- Compare simplified models (simulation / analytical) with real ferromagnetic materials
- Calculate demagnetisation matrices out of measurements

VSM Measurements for various helices (Magnetic Moment)

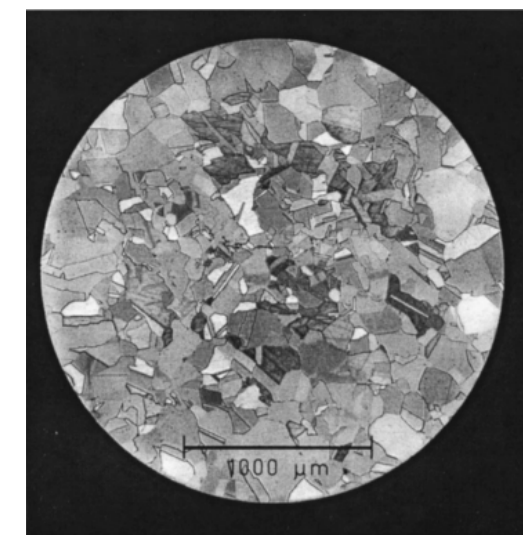
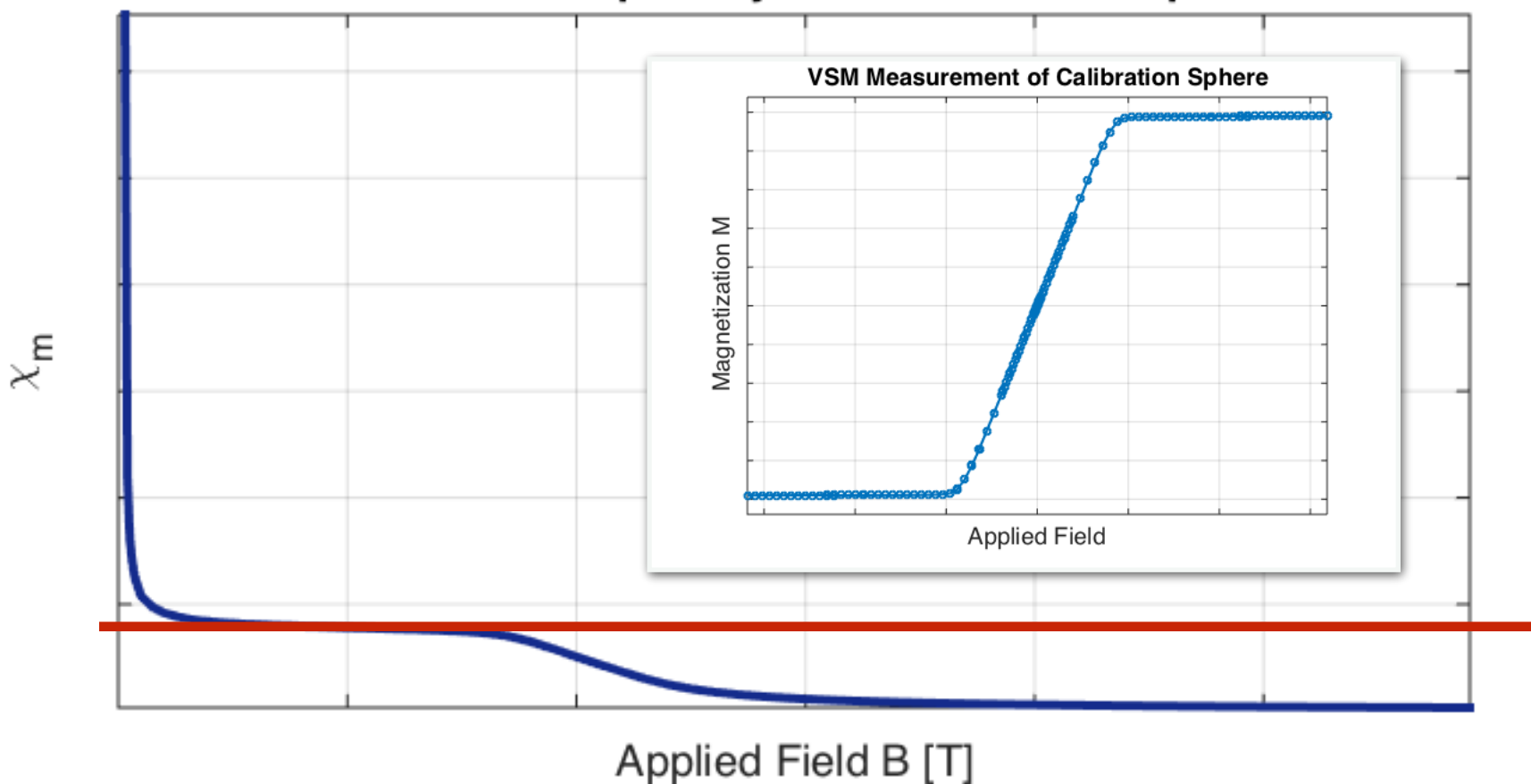


Analysis for Low Fields



$$\chi_a = \begin{pmatrix} dM_{rad,rad} & 0 & dM_{ax,rad} \\ 0 & dM_{rad,rad} & dM_{ax,rad} \\ dM_{rad,ax} & dM_{rad,ax} & dM_{ax,ax} \end{pmatrix}$$

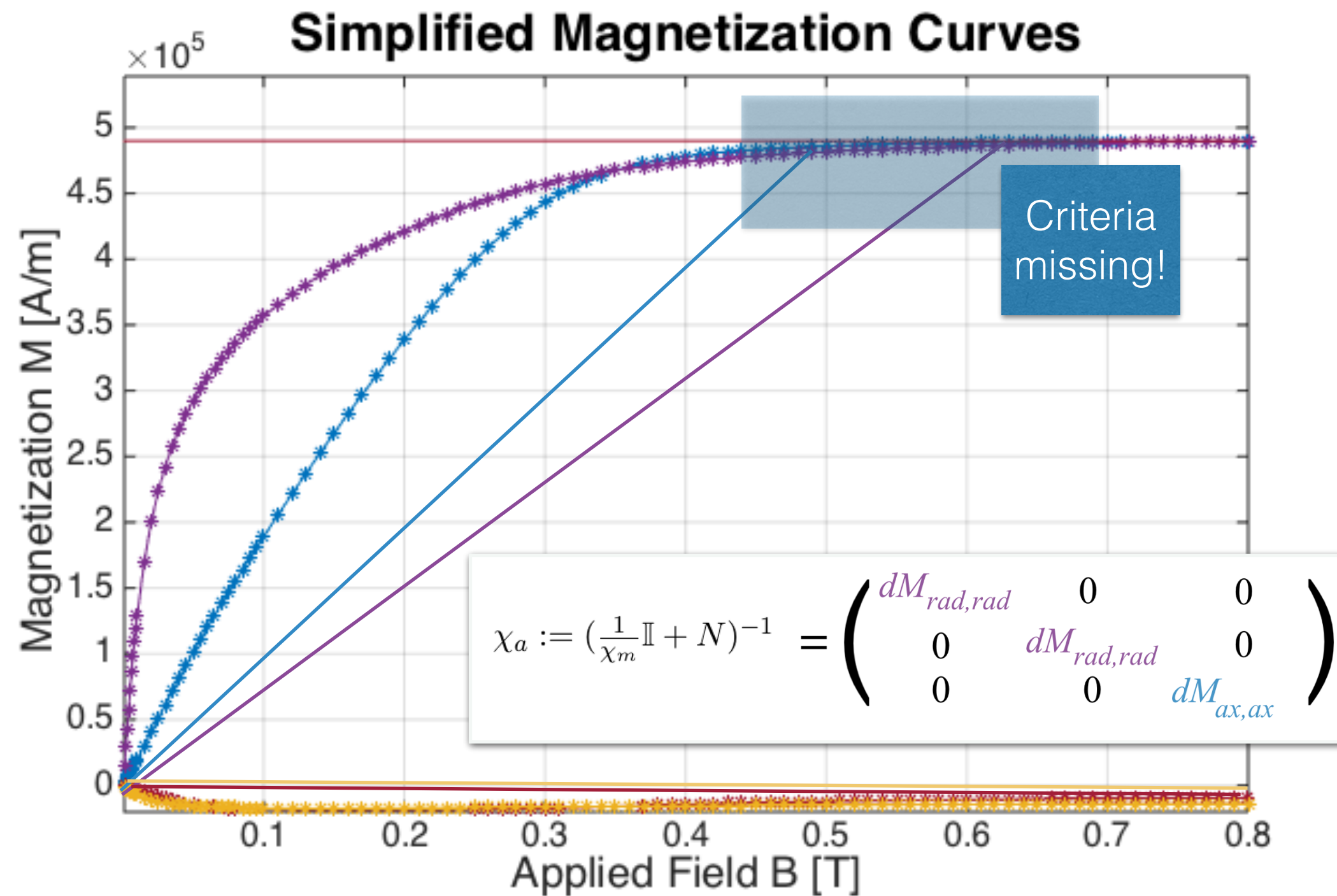
Intrinsic Susceptibility from Calibration Sphere



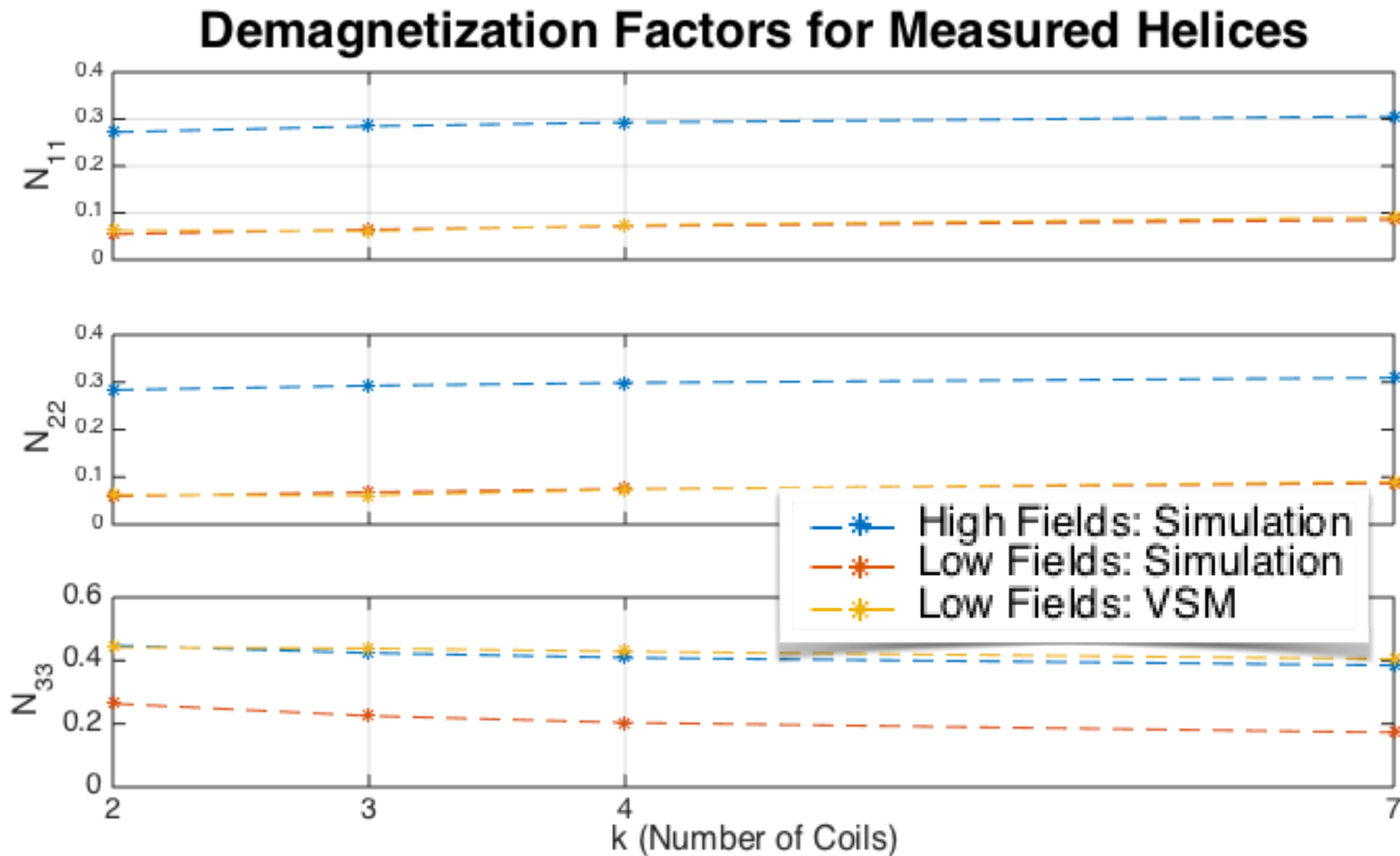
$$\chi_m \approx 24$$

Shull, R. D., McMichael, R. D., Swartzendruber, L. J., & Leigh, S. D. (2000). Absolute magnetic moment measurements of nickel spheres. *Journal of Applied Physics*, 87(9), 5992. doi:10.1063/1.372590

Analysis for High Fields



Results



Conclusions

- Through FEM, analytical models, and experiments we proposed two different regimes of magnetization for non-ellipsoidal structures
- Analysed the magnetic anisotropy of different helices as a function of coiling
- Developed a solid theory for further research:
 - Magnetisation of slender rods
 - Real time magnetic model for control

Further research

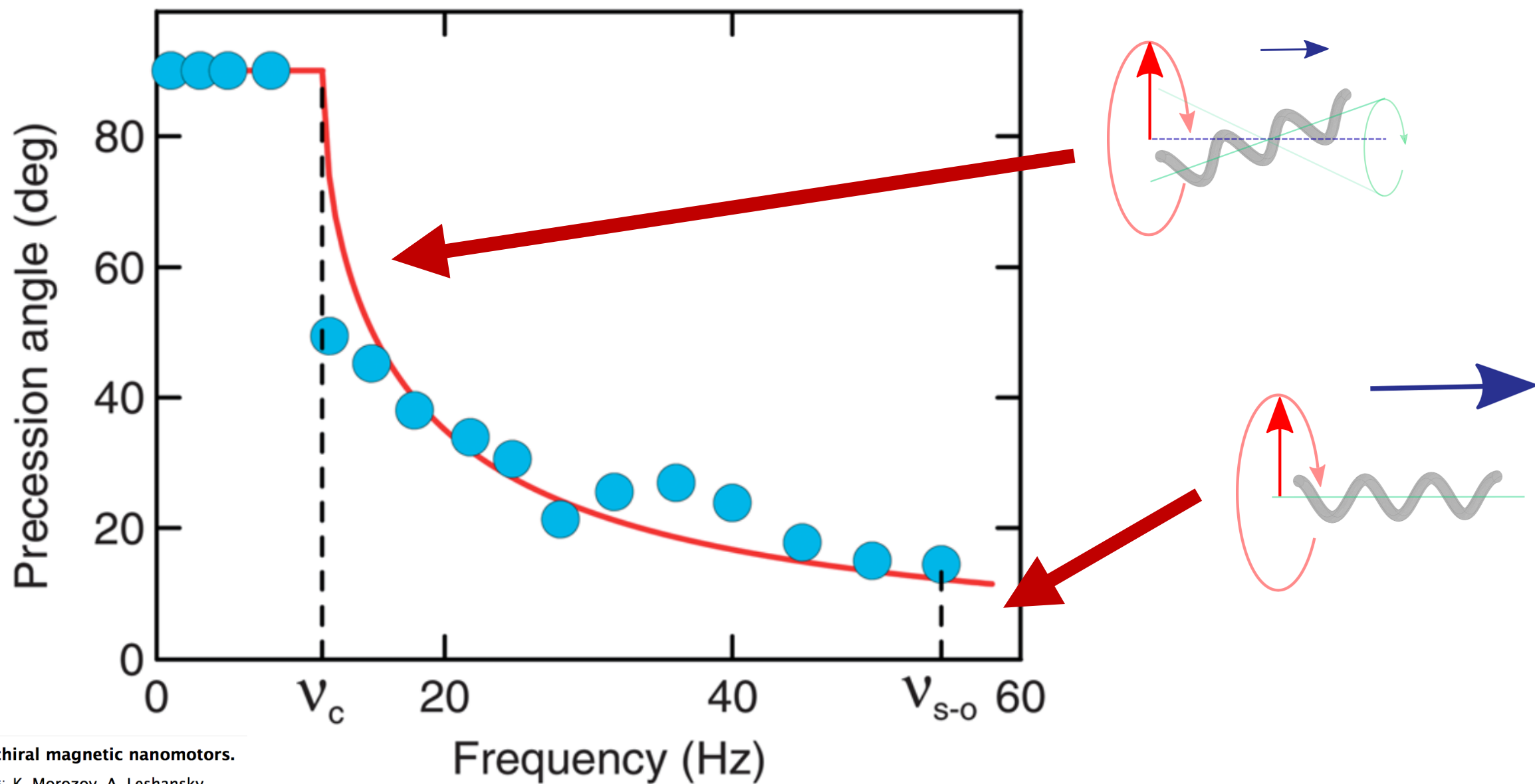
- Mathematical characteristics of low field demagnetisation factor
- Solving of the analytical model for low fields
 - Analysing characteristics of the demagnetisation factor on slender rods
 - Implementing suitable numerical methods (prone to singularities/ very high computational requirements if no simplifications)
- From VSM measurements:
 - Developing criteria to determine where the magnetisation reaches saturation point (smooth curves)
 - Developing more criteria to simplify hysteresis model and determine where the linear region is

Thank you!

Appendix

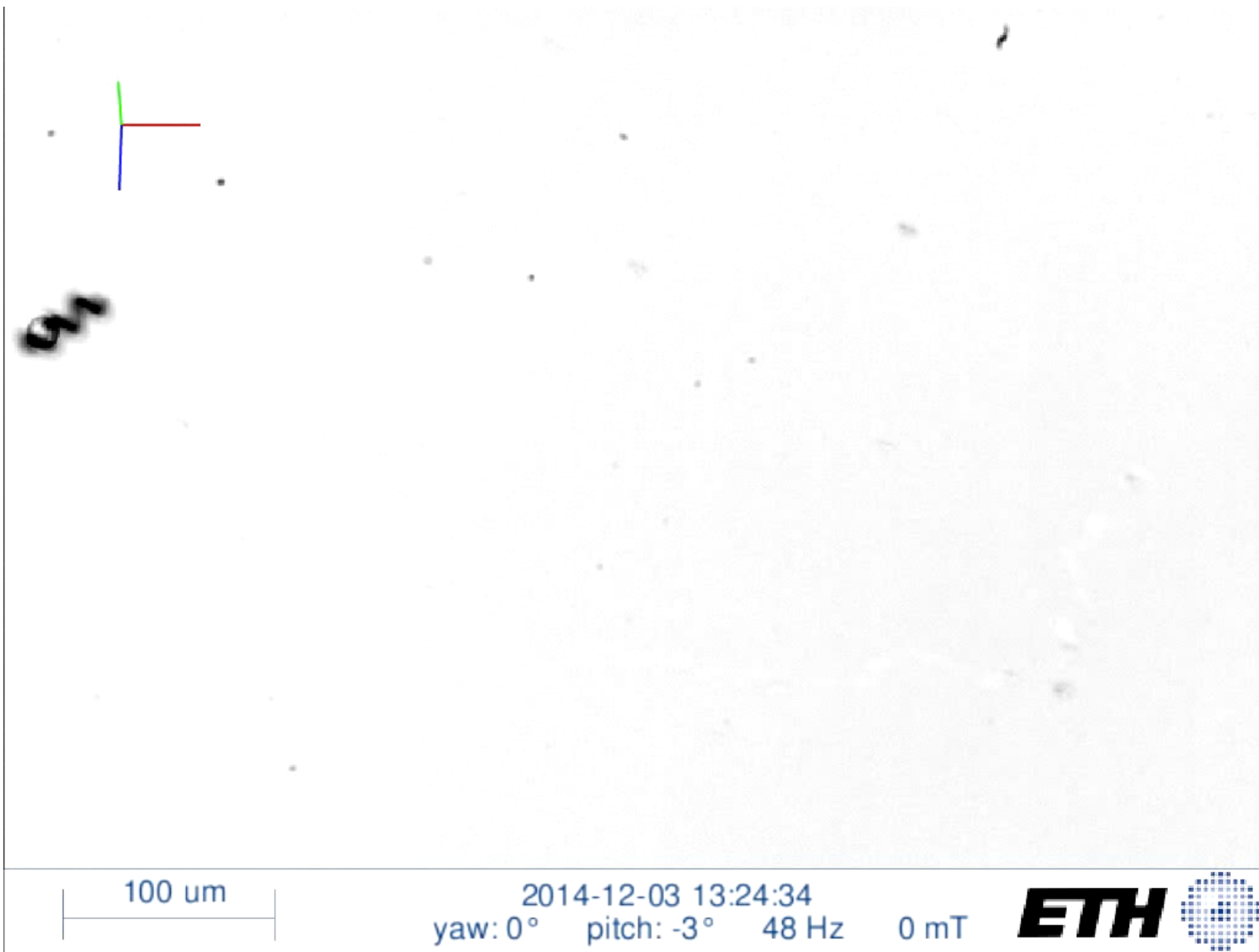
Precession Angle (Back up)

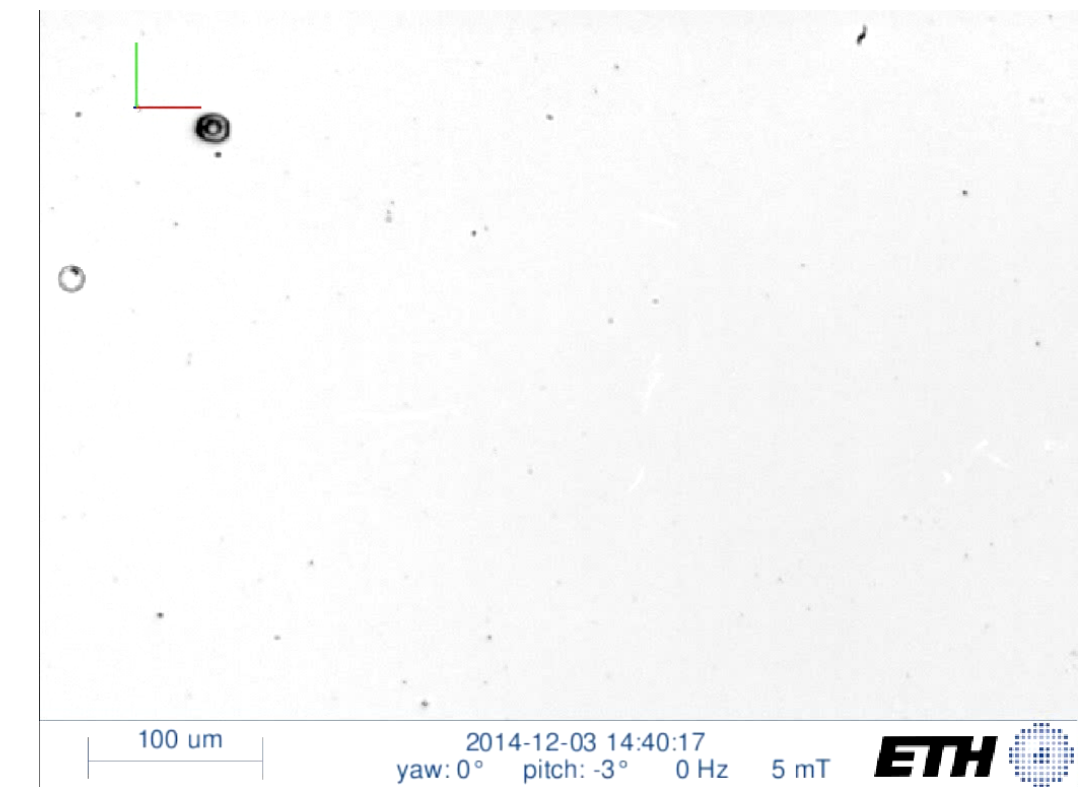
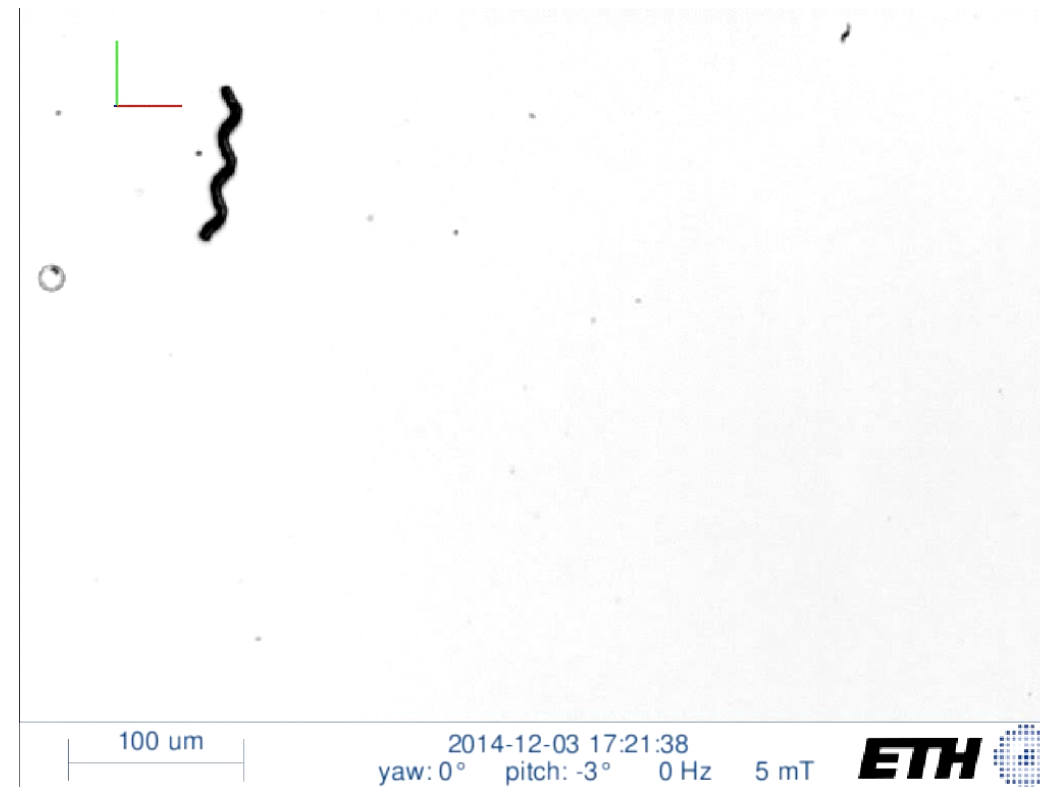
- Precession angle



The chiral magnetic nanomotors.

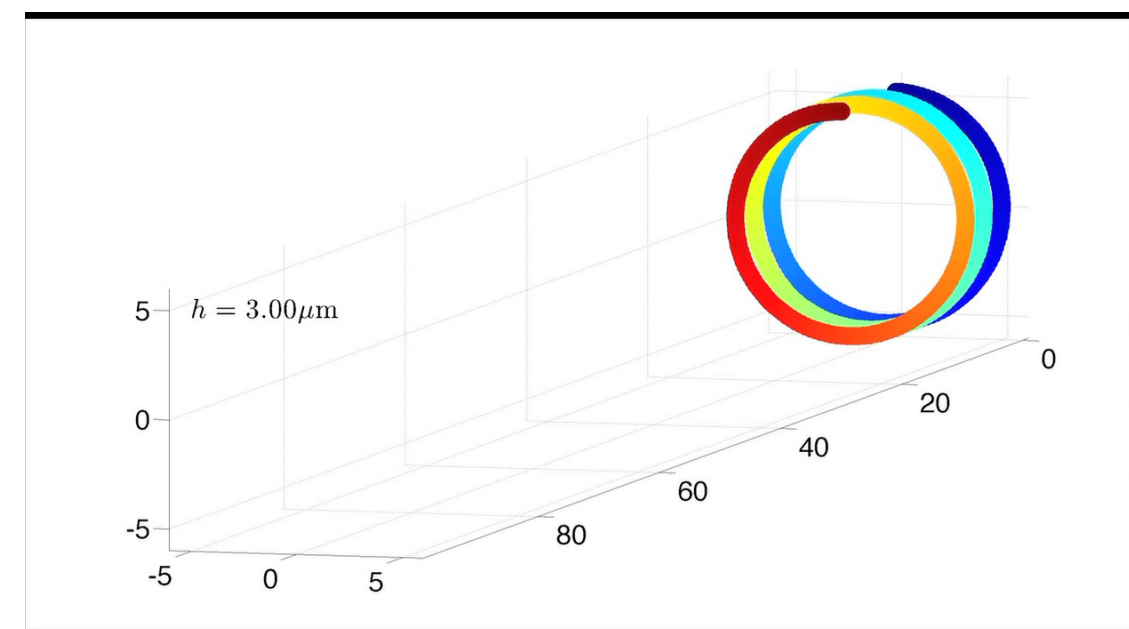
Authors: K. Morozov, A. Leshansky





Magnetism

- Alignment of the soft magnetic helix depends on magnetic properties!
 - Material
 - Shape (helix parameters)
- Experiments are available.
- Theoretic models only few:
 - Slender body approximation (Morozov, Leshansky)
 - *Only reliable for elongated shapes!*
 - Chains of beads
 - Only reliable for elongated shapes

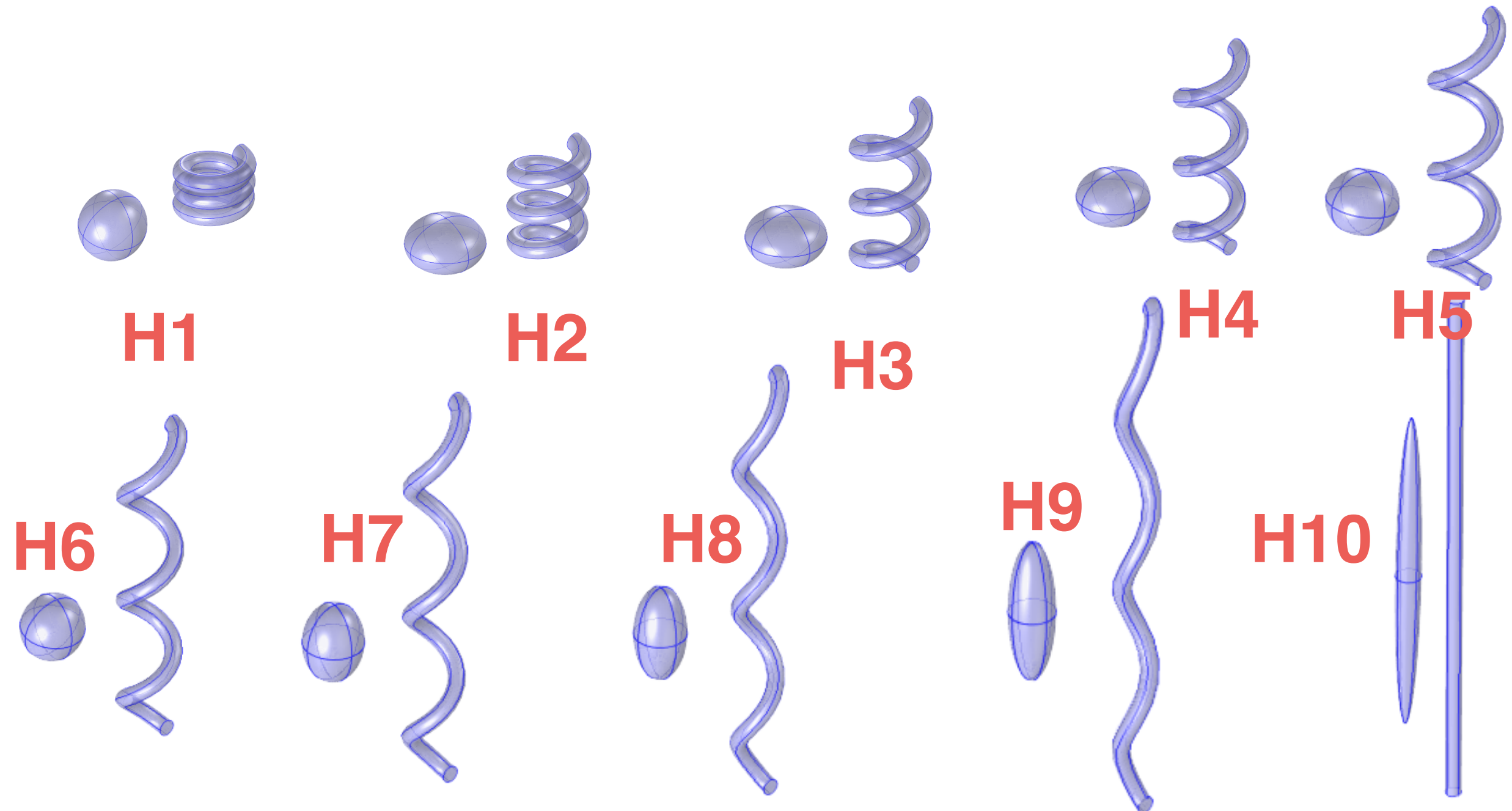


Magnetization directions and geometries of helical microswimmers for linear velocity-frequency response

Authors: H. Fu, M. Jabbarzadeh, F. Meshkati

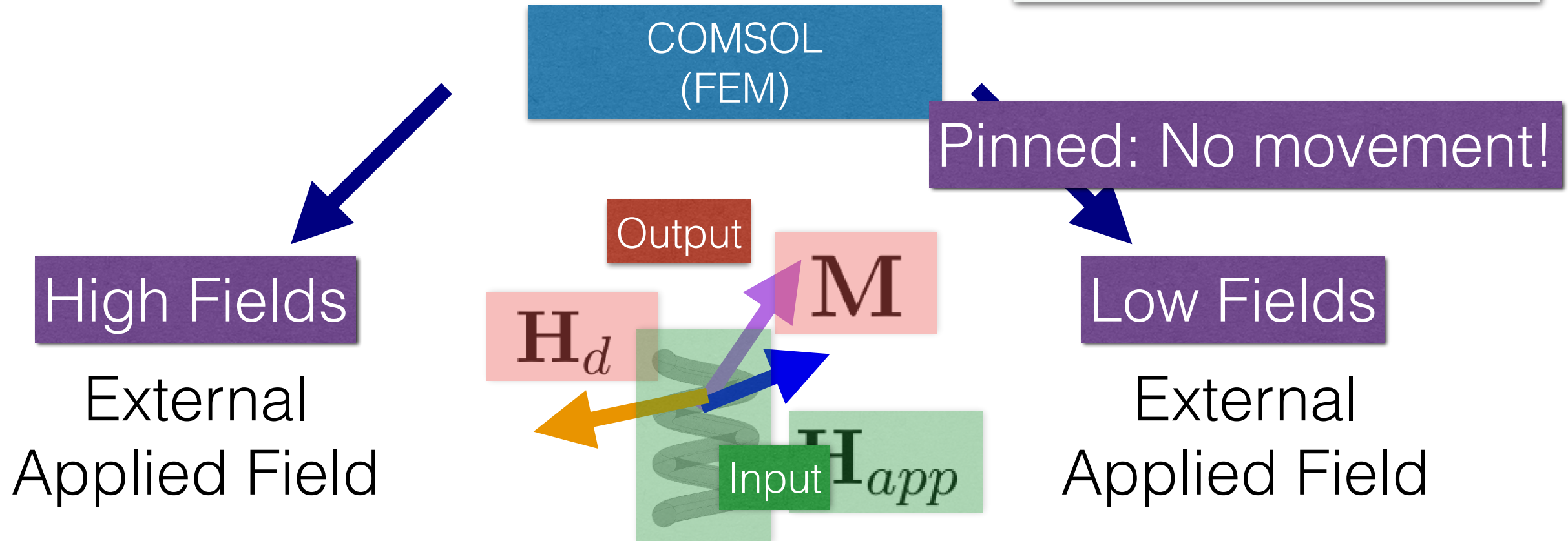
Dynamical configurations and bistability of helical nanostructures under external torque, Arijit Ghosh, Debadrita Paria, Haobijam Johnson Singh, Pooyath Lekshmy Venugopalan, and Ambarish Ghosh

Equivalent Ellipsoids (Full Magnetic)

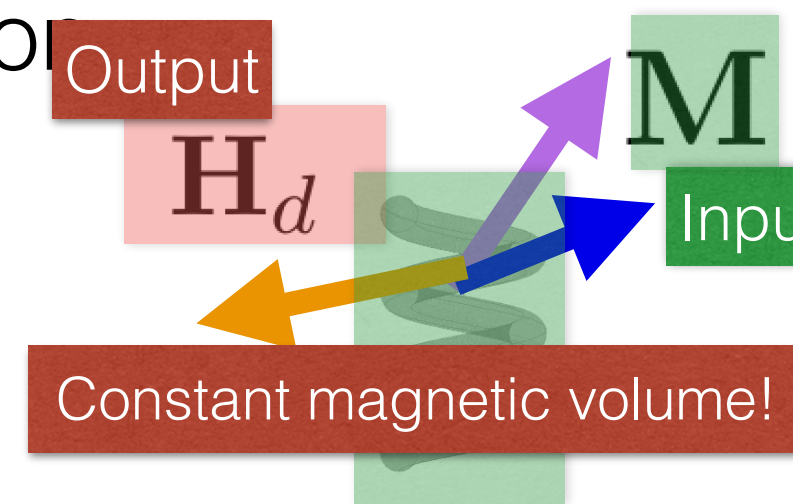


Simulations

$$\chi_m = 1000$$



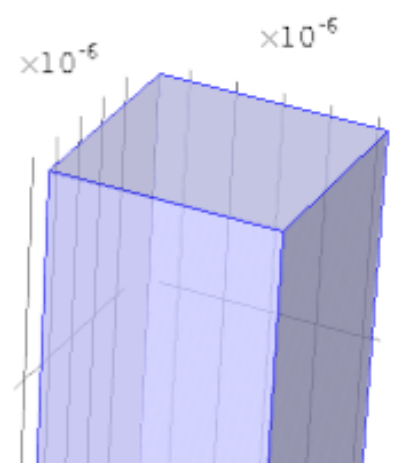
Given magnetisation
(Saturation)



Simulation (High Fields) vs Analytical (Block)

`N_simulationM =`

$$\begin{matrix} 0.4285 & -0.0003 & 0.0002 \\ -0.0003 & 0.4282 & -0.0002 \\ 0.0002 & -0.0002 & 0.0995 \end{matrix}$$



`N`

$$\begin{aligned} \pi D_z = & \frac{b^2 - c^2}{2bc} \ln\left(\frac{\sqrt{a^2 + b^2 + c^2} - a}{\sqrt{a^2 + b^2 + c^2} + a}\right) + \frac{a^2 - c^2}{2ac} \ln\left(\frac{\sqrt{a^2 + b^2 + c^2} - b}{\sqrt{a^2 + b^2 + c^2} + b}\right) + \frac{b}{2c} \ln\left(\frac{\sqrt{a^2 + b^2} + a}{\sqrt{a^2 + b^2} - a}\right) + \frac{a}{2c} \ln\left(\frac{\sqrt{a^2 + b^2} + b}{\sqrt{a^2 + b^2} - b}\right) \\ & + \frac{c}{2a} \ln\left(\frac{\sqrt{b^2 + c^2} - b}{\sqrt{b^2 + c^2} + b}\right) + \frac{c}{2b} \ln\left(\frac{\sqrt{a^2 + c^2} - a}{\sqrt{a^2 + c^2} + a}\right) + 2 \arctan\left(\frac{ab}{c\sqrt{a^2 + b^2 + c^2}}\right) + \frac{a^3 + b^3 - 2c^3}{3abc} \\ & + \frac{a^2 + b^2 - 2c^2}{3abc} \sqrt{a^2 + b^2 + c^2} + \frac{c}{ab} (\sqrt{a^2 + c^2} + \sqrt{b^2 + c^2}) - \frac{(a^2 + b^2)^{3/2} + (b^2 + c^2)^{3/2} + (c^2 + a^2)^{3/2}}{3abc}. \end{aligned}$$

Aharoni, A. (1998). Demagnetizing factors for rectangular ferromagnetic prisms. J. Appl. Phys. doi: 10.1063/1.367113

$$N = -\frac{1}{4\pi} \int_V \left(\mathbf{n}(\mathbf{r}') \frac{(\mathbf{r}' - \mathbf{r})^T}{|\mathbf{r}' - \mathbf{r}|^3} \right) \mathbb{I} d^3 r'$$

$$N(\mathbf{r}) = \Psi(\mathbf{r})^{-1} - \frac{1}{\chi_m} \mathbb{I}$$

$$\frac{1}{\chi_m} \Psi(\mathbf{r}) = -\mathcal{N}(\mathbf{r}, \Psi(\mathbf{r})) + \mathbb{I}$$

High Fields

\mathbf{H}_d

$$\mathbf{H}(\mathbf{r}) = -\frac{1}{4\pi} \int_{\partial V} \left(\mathbf{n}(\mathbf{r}') \frac{(\mathbf{r}' - \mathbf{r})^T}{|\mathbf{r}' - \mathbf{r}|^3} \right) \mathbf{M}(\mathbf{r}') d^3 r' + \mathbf{H}_{app}$$

$$\mathbf{H}_d(\mathbf{r}) = -\frac{1}{4\pi} \int_{\partial V} \left(\mathbf{n}(\mathbf{r}') \frac{(\mathbf{r}' - \mathbf{r})^T}{|\mathbf{r}' - \mathbf{r}|^3} \right) \mathbf{M}(\mathbf{r}') d^3 r' \quad \mathbf{M}(\mathbf{r}') = \mathbf{M}_s$$



$$\mathbf{H}_d(\mathbf{r}) = -\frac{1}{4\pi} \int_{\partial V} \left(\mathbf{n}(\mathbf{r}') \frac{(\mathbf{r}' - \mathbf{r})^T}{|\mathbf{r}' - \mathbf{r}|^3} \right) \mathbb{I} d^3 r' \mathbf{M}_s$$

Saturated!

N

$$\mathbf{H}_d = -N \mathbf{M}_s$$

$$N = -\frac{1}{4\pi} \int_{\partial V} \left(\mathbf{n}(\mathbf{r}') \frac{(\mathbf{r}' - \mathbf{r})^T}{|\mathbf{r}' - \mathbf{r}|^3} \right) \mathbb{I} d^3 r'$$

Low Fields

$$\mathbf{H}(\mathbf{r}) = -\frac{1}{4\pi} \int_V \left(\mathbf{n}(\mathbf{r}') \frac{(\mathbf{r}' - \mathbf{r})^T}{|\mathbf{r}' - \mathbf{r}|^3} \right) \mathbf{M}(\mathbf{r}') d^3r' + \mathbf{H}_{app}$$

$$\mathbf{M} = \mathbf{f}(\mathbf{H})$$

↓ No hysteresis (simplification)

$$\mathbf{M} = \chi_m(\mathbf{H}) \mathbf{H}$$

↓ Linearisation (constant slope)

$$\mathbf{M} = \chi_m \mathbf{H}$$



$$\mathbf{H}(\mathbf{r}) = -\mathcal{N}(\mathbf{r}, \mathbf{M}) + \mathbf{H}_{app}$$



$$\frac{1}{\chi_m} \mathbf{M}(\mathbf{r}) = -\mathcal{N}(\mathbf{r}, \mathbf{M}(\mathbf{r})) + \mathbf{H}_{app}$$

χ_m

scalar
(crystalline isotropy)

$$\frac{1}{\chi_m} \mathbf{M}(\mathbf{r}) = -\mathcal{N}(\mathbf{r}, \mathbf{M}(\mathbf{r})) + \mathbf{H}_{\text{app}}$$

Linear Solutions!

$$\mathbf{M}(\mathbf{r}) = \Psi(\mathbf{r}) \mathbf{H}_{\text{app}}$$

$$\frac{1}{\chi_m} \Psi(\mathbf{r}) = -\mathcal{N}(\mathbf{r}, \Psi(\mathbf{r})) + \mathbb{I}$$

$$N(\mathbf{r}) = -H_d(\mathbf{r}) M(\mathbf{r})^{-1} \longrightarrow N(\mathbf{r}) = \Psi(\mathbf{r})^{-1} - \frac{1}{\chi_m} \mathbb{I}$$

3D surface integral matrix equation

$$\frac{1}{\chi_m} \Psi(\mathbf{r}) = -\mathcal{N}(\mathbf{r}, \Psi(\mathbf{r})) + \mathbb{I}$$

$$N(\mathbf{r}) = \Psi(\mathbf{r})^{-1} - \frac{1}{\chi_m} \mathbb{I}$$

simplifications



Line integral:
Fourier
Legendre

Not successful!

Sophisticated
numerical methods
needed